Transverse quantum decoherence of a fast particle in a gas

David Gaspard and Jean-Marc Sparenberg
Nuclear Physics and Quantum Physics, CP229, Université libre de Bruxelles (ULB), 1050 Brussels, Belgium

(Received 8 December 2022; accepted 3 February 2023; published 15 February 2023)

The decoherence of a fast quantum particle in a gas is studied by applying the Kramers-Moyal expansion to the quantum master equation for the reduced density matrix of the particle. This expansion leads to a general form of the Caldeira-Leggett master equation accounting for the angular variation of the differential cross section. The equation describes the decoherence in both the longitudinal and transverse directions with respect to the particle motion. It is shown that, when the differential cross section is concentrated in the forward direction, transverse decoherence dominates. The coherence region off the diagonal of the density matrix is characterized by coherence lengths, which can be deduced, for Gaussian states, from the momentum covariance matrix according to a Heisenberg-type uncertainty relation. Finally, the longitudinal-to-transverse ratio of the coherence lengths is estimated for an α particle of a few MeVs. This ratio indicates that the coherence region looks like an ellipsoid elongated in the direction of motion.

DOI: 10.1103/PhysRevA.107.022214

I. INTRODUCTION

The question of the propagation of a quantum particle in a detector, such as a cloud chamber or an ionization chamber, is probably one of the least obvious ever addressed from first principles. It was originally asked by Darwin [1] and Mott [2] in the early years of quantum theory. The problem at the time was to understand how the appearance of linear tracks of α particles in cloud chambers could be consistent with the quantum-mechanical description of these particles as waves. In his paper, Mott gave a relevant explanation of this phenomenon by accounting for the whole Hilbert space generated by the excitation states of the detector constituents. His explanation is still verified today in recent works [3–9].

An important issue pointed out by Darwin and Mott resides in the lack of information about the state of the α particle provided by single-particle quantum measurements. In particular, although the wave function of the α particle is depicted as symmetrical around the radioactive source, individual tracks seem to have preferred directions [1,2], in apparent contradiction with quantum mechanics. This comes from the probabilistic nature of the quantum-mechanical wave function and the inherent difficulty of its interpretation. However, the specific issue of interpretation is not the subject of the present paper. Instead, this work attempts to describe on average the whole ensemble of possible measurement outcomes using the reduced density matrix of the particle. It has been known since the pioneering work of Joos and Zeh [10–12] that the reduced density matrix of a particle undergoes decoherence, which is the exponential decay of its off-diagonal elements, due to the interaction with the quantum environment [13–17]. This effect is considered as the signature of quantum measurement and the transition from quantum to classical behaviors [12,18–22]. Until now, decoherence theory has been successfully observed in numerous experiments on large slow molecules [23–30], but not on fast incident particles.

The purpose of the present paper is to study the quantum master equation derived in a previous paper [31] and to specialize it to the context of a fast particle passing through a detector modeled as a gas of slow particles. As in the previous paper [31], the interaction potential between the incident particle and the gas particles is assumed to be short range, hence neglecting the Coulombic nature of the collisions with the electrons [32–36]. Despite this approximation, the differential cross section in the center-of-mass frame is supposed to be focused enough in the forward direction to avoid significant deviation of the particle from its initial direction [37,38]. This latter assumption enables the use of a quantum-mechanical analog of the Kramers-Moyal expansion [39–42] to approximate the collisional term of the master equation. This procedure leads to an equation similar to the master equation found by Caldeira and Leggett [16,17,43–46] with drift and diffusion terms acting in momentum space, but of a more general kind, because it does not assume that the particle is slow compared to the gas. In the Wigner representation, this master equation reduces to a Fokker-Planck equation for the momentum distribution of the particle. Using a definition for the coherence length [47], it will be shown that, due to the assumption of small deflection of the particle, decoherence dominates in the direction transverse to motion. Therefore, the coherent wave packet looks like an ellipsoid elongated in the direction of motion.

This paper is organized as follows. The quantum master equation of Ref. [31] governing the reduced density matrix of the particle is presented in Sec. II. The general properties of this equation, including thermalization and spatial decoherence, are considered in Secs. II A and II B, respectively. These general properties do not rely on the Kramers-Moyal approximation. Then approximate expressions based on the Kramers-Moyal expansion are derived in Sec. III. In particular, after the calculation of the moments that takes place in Sec. III A, a general form of the Caldeira-Leggett master

equation is presented in Sec. III B. This equation is then specialized to the case of strong forward scattering in Sec. III B 1 and expressed in terms of the angular momentum operator to shed light on the spherical nature of transverse decoherence. Additional explanations about the appearance of the angular momentum operator are given in the Appendix. The Wigner transform of the master equation is then established in Sec. III B 2. In Sec. IV a coherence length matrix is introduced to characterize the region of coherence around the diagonal of the reduced density matrix. It is shown in Sec. IV A that, for the Gaussian states predicted by the Fokker-Planck equation, the coherence length is the inverse of the standard deviation of the momentum. This is due to the existence of a Heisenberg-type uncertainty relation between the coherence length and the momentum. Finally, this relation leads to an approximate solution for the time evolution of the coherence length which is obtained in Sec. IV C based on the calculations of Sec. IV B.

Throughout this paper, SI units are used with the recommended values of Ref. [48] for the fundamental constants. Regarding the notation, c is the speed of light in vacuum, h is the Planck constant, $\hbar = h/2\pi$ is the reduced Planck constant, α is the fine-structure constant, and $k_{\rm B}$ is the Boltzmann constant. All the calculations will be performed for an arbitrary number of spatial dimensions: $d \in \{2, 3, 4, \ldots\}$. Quantum operators will be denoted by $\hat{A}$ to distinguish them from the associated eigenvalue A.

II. GENERAL PROPERTIES OF THE MASTER EQUATION

One considers a model for a spinless quantum particle of mass m_a interacting with a thermal bath of N mobile scatterers of mass m_b in a cubic enclosure denoted by $\mathcal{V}$ of side L and volume $V = L^d$. The Hamiltonian of the whole system reads [31]

$$\hat{H} = \underbrace{\frac{\hbar^2\hat{\mathbf{k}}_a^2}{2m_a}}_{\hat{H}_a} + \underbrace{\sum_{i=1}^{N}\frac{\hbar^2\hat{\mathbf{k}}_i^2}{2m_b}}_{\hat{H}_b} + \underbrace{\sum_{i=1}^{N} u(\hat{\mathbf{r}} - \hat{\mathbf{x}}_i)}_{\hat{U}}, \tag{1}$$

where $(\hat{\mathbf{r}}, \hat{\mathbf{k}}_a)$ are the position and the momentum of the particle, and $(\hat{\mathbf{x}}_1, \hat{\mathbf{x}}_2, \ldots, \hat{\mathbf{x}}_N)$ and $(\hat{\mathbf{k}}_1, \hat{\mathbf{k}}_2, \ldots, \hat{\mathbf{k}}_N)$ are the positions and the momenta of the scatterers, respectively. These momenta are quantized to the cubic lattice

$$\mathbf{k} = \frac{2\pi}{L}(n_1, \ldots, n_d)^{\intercal} \quad \forall\, (n_1, \ldots, n_d) \in \mathbb{Z}^d \tag{2}$$

due to the periodic boundary conditions over the wave function. The number density of scatterers, $n = N/V$, is supposed to be fixed, even in the continuum limit for the momentum states, namely, $V \to \infty$. In addition, the potential $u(\mathbf{r})$ is assumed to be spherically symmetric and of short range.

It was shown in a previous paper [31] that the master equation for the reduced density matrix of the particle, defined as the partial trace over the bath of the full density matrix

$$\hat{\rho}_a(t) = \mathrm{Tr}_b\hat{\rho}(t), \tag{3}$$

has the form

$$\frac{\partial\hat{\rho}_a}{\partial t} = \mathcal{L}_a\hat{\rho}_a + \mathcal{R}_a\hat{\rho}_a. \tag{4}$$

The symbol $\mathcal{L}_a$ in Eq. (4) stands for the Liouvillian superoperator

$$\mathcal{L}_a\hat{\rho}_a = \frac{1}{i\hbar}[\hat{H}_a, \hat{\rho}_a], \tag{5}$$

which describes the free propagation of the particle, and $\mathcal{R}_a$ is the Redfieldian superoperator, or dissipator [45], which reads [31]

$$\mathcal{R}_a\hat{\rho}_a = \frac{1}{2}\sum_{\mathbf{q}}(e^{i\mathbf{q}\cdot\hat{\mathbf{r}}}\{\hat{W}_{\mathbf{q}}, \hat{\rho}_a\}e^{-i\mathbf{q}\cdot\hat{\mathbf{r}}} - \{\hat{W}_{\mathbf{q}}, \hat{\rho}_a\}), \tag{6}$$

where $\{\hat{A}, \hat{B}\} = \hat{A}\hat{B} + \hat{B}\hat{A}$ is the anticommutator. The dissipator (6) was derived in the previous paper [31] using the Markov assumption, the perturbative approximation, and the weak scattering condition [49,50]

$$k_{a,0}\ell_{\rm s} \gg 1, \tag{7}$$

where $k_{a,0} = 2\pi/\lambda_{a,0}$ is the initial particle wave number and $\ell_{\rm s} = (n\sigma)^{-1}$ is the mean free path, σ being the total collision cross section. It was shown in that paper that the Redfield equation (4)–(6) approximately reduces to the Boltzmann equation in the Wigner representation. In this respect, it is similar to the quantum linear Boltzmann equation of Refs. [14,15,17], although it cannot be cast into the Lindblad form.

In Eq. (6), $\hat{W}_{\mathbf{q}}$ denotes the total collision rate operator associated with the transferred momentum $\mathbf{q}$ and is given by

$$\hat{W}_{\mathbf{q}} = W_{\mathbf{q}}(\hat{\mathbf{k}}_a) = N\langle w_{\mathbf{q}}(\hat{\mathbf{k}}_a, \hat{\mathbf{k}}_b)\rangle_b, \tag{8}$$

where $\langle\cdot\rangle_b$ stands for the average over the momentum $\mathbf{k}_b$ of some generic bath particle. This average is defined as

$$\langle X(\hat{\mathbf{k}}_a, \hat{\mathbf{k}}_b)\rangle_b = \int_{\mathbb{R}^d} d\mathbf{k}_b f_b(\mathbf{k}_b) X(\hat{\mathbf{k}}_a, \mathbf{k}_b) \tag{9}$$

and is still an operator acting on particle a. In Eq. (9), $f_b(\mathbf{k}_b)$ is the single-particle momentum distribution of the bath normalized according to $\int_{\mathbb{R}^d} d\mathbf{k}_b f_b(\mathbf{k}_b) = 1$. The gas is supposed to be in the rest frame so that the average velocity is zero: $\langle\mathbf{k}_b\rangle_b = \mathbf{0}$.

In Eq. (8), $w_{\mathbf{q}}(\hat{\mathbf{k}}_a, \hat{\mathbf{k}}_b)$ is the binary collision rate operator for a fixed value of $\hat{\mathbf{k}}_b$. At leading order of perturbation theory in the potential $u(\mathbf{r})$, this operator is given by

$$w_{\mathbf{q}}(\hat{\mathbf{k}}_a, \hat{\mathbf{k}}_b) = \frac{2\pi}{\hbar}\frac{1}{V^2}|\bar{u}(\mathbf{q})|^2\delta(\hat{D}_{\mathbf{q}}), \tag{10}$$

with the energy difference operator defined as

$$\hat{D}_{\mathbf{q}} = E_{\hat{\mathbf{k}}_a+\mathbf{q}} + E_{\hat{\mathbf{k}}_b-\mathbf{q}} - E_{\hat{\mathbf{k}}_a} - E_{\hat{\mathbf{k}}_b}. \tag{11}$$

In Eq. (11), $E_{\hat{\mathbf{k}}_a} = \frac{\hbar^2\hat{\mathbf{k}}_a^2}{2m_a}$ and $E_{\hat{\mathbf{k}}_b} = \frac{\hbar^2\hat{\mathbf{k}}_b^2}{2m_b}$ are convenient representations of the free Hamiltonians of the particle and the generic bath scatterer, respectively. The binary collision rate (10) is schematically represented in Fig. 1 in the space of the transferred momentum $\mathbf{q}$ for a fixed value of $\mathbf{k}_a$ and for $\mathbf{k}_b = \mathbf{0}$. The binary collision rate (10) is the product of the energy conservation Dirac delta $\delta(D_{\mathbf{q}})$, constraining $\mathbf{q}$ to a sphere, and the function $|\bar{u}(\mathbf{q})|^2$ centered at $\mathbf{q} = \mathbf{0}$.

In the continuum limit ($V \to \infty$), all the sums over the transferred momentum can be expressed in terms of the

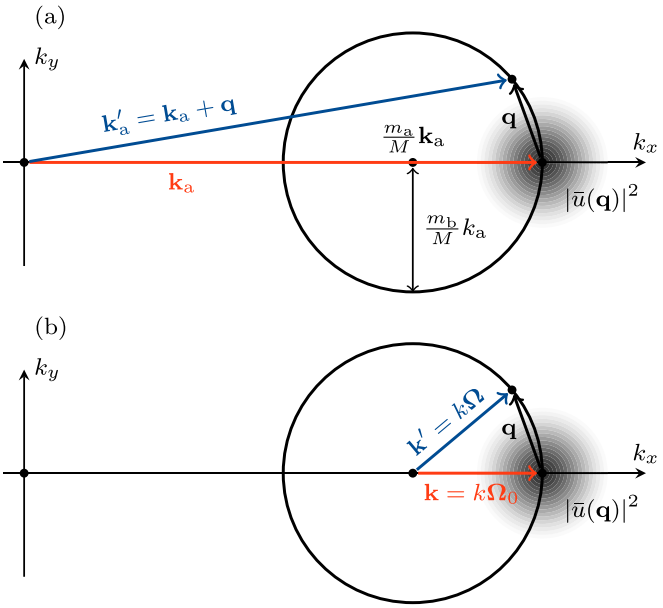

FIG. 1. Distribution of the final momentum $\mathbf{k}'_a = \mathbf{k}_a + \mathbf{q}$ of particle a after a single collision according to Eqs. (8) and (10), assuming the target scatterer is initially at rest ($\mathbf{k}_b = \mathbf{0}$), in (a) the laboratory frame and (b) the center-of-mass frame described by the relative momenta $\mathbf{k}$ and $\mathbf{k}'$. The mass ratio is $\frac{m_a}{m_b} = 3$. The circle represents the spherical energy shell $\delta(D_\mathbf{q})$ and the blurry function represents $|\bar{u}(\mathbf{q})|^2$ in Eq. (10).

differential cross section $\frac{d\sigma}{d\Omega}$ according to the property [31]

$$\sum_{\mathbf{q}} W_\mathbf{q}(\mathbf{k}_a)F(\mathbf{q}) = \oint_{\mathcal{S}_d} d\Omega \left\langle nv\frac{d\sigma}{d\Omega}(\mathbf{\Omega}|k\mathbf{\Omega}_0)F(k\mathbf{\Omega} - k\mathbf{\Omega}_0)\right\rangle_b, \tag{12}$$

which holds for any function $F(\mathbf{q})$ by definition of the differential cross section. The property (12) will be often used throughout this paper. On the right-hand side of Eq. (12), $\mathbf{k} = k\mathbf{\Omega}_0$ is the relative momentum between the colliding particles defined as

$$\mathbf{k} = \frac{m_b\mathbf{k}_a - m_a\mathbf{k}_b}{m_a + m_b}, \tag{13}$$

$\mathbf{v} = v\mathbf{\Omega}_0$ is the relative velocity

$$\mathbf{v} = \mathbf{v}_a - \mathbf{v}_b = \frac{\hbar\mathbf{k}_a}{m_a} - \frac{\hbar\mathbf{k}_b}{m_b} = \frac{\hbar\mathbf{k}}{m}, \tag{14}$$

and $\mathbf{\Omega}_0$ and $\mathbf{\Omega}$ are the initial and final directions, respectively, of the relative motion between the particle and the bath scatterer, as shown in Fig. 1(b). They are both normalized to unity: $\|\mathbf{\Omega}_0\| = \|\mathbf{\Omega}\| = 1$. In Eq. (14), m is the reduced mass of the binary system

$$m = \frac{m_a m_b}{m_a + m_b}. \tag{15}$$

In addition, we also define the total mass of the binary system for notational convenience

$$M = m_a + m_b. \tag{16}$$

Finally, it should be noted that the average over the bath $\langle\cdot\rangle_b$ in Eq. (12) concerns all the variables depending on $\mathbf{k}_b$, namely, v, k, and $\mathbf{\Omega}_0$ in particular.

A. Energy transfer and thermalization

In this section it is shown that the Redfield equation (4) leads to the thermalization of the particle. First, the governing equation for the mean particle energy $\langle E_{\mathbf{k}_a}\rangle_a = \mathrm{Tr}_a(E_{\hat{\mathbf{k}}_a}\hat{\rho}_a)$ is given by

$$\frac{d\langle E_{\mathbf{k}_a}\rangle_a}{dt} = \mathrm{Tr}_a\big(E_{\hat{\mathbf{k}}_a}\mathcal{R}_a\hat{\rho}_a\big), \tag{17}$$

since the contribution from the free propagation term $\mathcal{L}_a\hat{\rho}_a$ in Eq. (4) is zero due to energy conservation. Using the cyclic property of trace and the momentum translation property

$$e^{-i\mathbf{q}\cdot\hat{\mathbf{r}}}f(\hat{\mathbf{k}}_a)e^{i\mathbf{q}\cdot\hat{\mathbf{r}}} = f(\hat{\mathbf{k}}_a + \mathbf{q}), \tag{18}$$

we get, from Eqs. (6) and (17),

$$\frac{d\langle E_{\mathbf{k}_a}\rangle_a}{dt} = \mathrm{Tr}_a\left(\frac{1}{2}\sum_{\mathbf{q}}\{\hat{W}_\mathbf{q}, \hat{\rho}_a\}\big(E_{\hat{\mathbf{k}}_a+\mathbf{q}} - E_{\hat{\mathbf{k}}_a}\big)\right). \tag{19}$$

In addition, since the commutation $[\hat{W}_\mathbf{q}, E_{\hat{\mathbf{k}}_a}] = 0$ holds, we can write

$$\frac{d\langle E_{\mathbf{k}_a}\rangle_a}{dt} = \mathrm{Tr}_a\left(\hat{\rho}_a\sum_{\mathbf{q}}\hat{W}_\mathbf{q}\big(E_{\hat{\mathbf{k}}_a+\mathbf{q}} - E_{\hat{\mathbf{k}}_a}\big)\right). \tag{20}$$

Now we can use the property (12) to deal with the sum over $\mathbf{q}$ in Eq. (20). Thus, we get

$$\sum_{\mathbf{q}} W_\mathbf{q}(\mathbf{k}_a)\big(E_{\mathbf{k}_a+\mathbf{q}} - E_{\mathbf{k}_a}\big) = \oint_{\mathcal{S}_d} d\Omega\left\langle nv\frac{d\sigma}{d\Omega}(\mathbf{\Omega}|k\mathbf{\Omega}_0)\big(E_{\mathbf{k}_a+\mathbf{q}} - E_{\mathbf{k}_a}\big)\right\rangle_b, \tag{21}$$

assuming implicitly $\mathbf{q} = k(\mathbf{\Omega} - \mathbf{\Omega}_0)$ on the right-hand side. Introducing the energy transfer averaged over the differential cross section

$$T_a = \oint_{\mathcal{S}_d} d\Omega\frac{d\sigma}{d\Omega}(\mathbf{\Omega}|k\mathbf{\Omega}_0)\big(E_{\mathbf{k}_a+\mathbf{q}} - E_{\mathbf{k}_a}\big), \tag{22}$$

Eq. (20) can be rewritten more simply as

$$\frac{d\langle E_{\mathbf{k}_a}\rangle_a}{dt} = \mathrm{Tr}_a(\hat{\rho}_a\langle n\hat{v}\hat{T}_a\rangle_b) = \langle\langle n\hat{v}\hat{T}_a\rangle_b\rangle_a. \tag{23}$$

Then we expand the energy transfer integral (22) to get

$$T_a = \frac{\hbar^2}{2m_a}\oint_{\mathcal{S}_d} d\Omega\frac{d\sigma}{d\Omega}(\mathbf{\Omega}|k\mathbf{\Omega}_0)(\mathbf{q}^2 + 2\mathbf{k}_a\cdot\mathbf{q}). \tag{24}$$

To perform the integral (24), it is convenient to introduce the momentum-transfer cross section [51]

$$\sigma_{\mathrm{tr}}(k) = \oint_{\mathcal{S}_d} d\Omega\frac{d\sigma}{d\Omega}(\mathbf{\Omega}|k\mathbf{\Omega}_0)(1 - \mathbf{\Omega}\cdot\mathbf{\Omega}_0). \tag{25}$$

This quantity has the same units as the total cross section $\sigma(k)$ and is always bounded by $\sigma_{\mathrm{tr}} \in [0, \sigma]$. It mainly characterizes the dispersion of the center-of-mass differential cross section around the forward direction. When $\sigma_{\mathrm{tr}} \ll \sigma$, this means

that the cross section is peaked in the forward direction and that the particle undergoes small deflections upon collision. On the contrary, when $\sigma_{\rm tr} = \sigma$, the cross section is independent of the direction, i.e., isotropic, and the particle is strongly deflected.

Using the facts that $\mathbf{q} = k(\mathbf{\Omega} - \mathbf{\Omega}_0)$ and $\mathbf{k} = k\mathbf{\Omega}_0$, we find two exact integrals for the transferred momentum which derive from definition (25), namely,

$$\oint_{\mathcal{S}_d} d\Omega \frac{d\sigma}{d\Omega}(\mathbf{\Omega}|k\mathbf{\Omega}_0)\mathbf{q} = -\mathbf{k}\sigma_{\rm tr}(k) \tag{26}$$

and

$$\oint_{\mathcal{S}_d} d\Omega \frac{d\sigma}{d\Omega}(\mathbf{\Omega}|k\mathbf{\Omega}_0)\mathbf{q}^2 = 2\mathbf{k}^2\sigma_{\rm tr}(k). \tag{27}$$

Substituting Eqs. (26) and (27) into Eq. (24), we get

$$T_a = \sigma_{\rm tr}(k)\frac{\hbar^2}{m_a}(\mathbf{k}^2 - \mathbf{k}_a \cdot \mathbf{k}). \tag{28}$$

Using Eq. (13) to expand $\mathbf{k}$, Eq. (28) becomes

$$T_a = \sigma_{\rm tr}(k)\frac{\hbar^2}{M^2}\big[m_a\mathbf{k}_b^2 - m_b\mathbf{k}_a^2 + (m_a - m_b)\mathbf{k}_a \cdot \mathbf{k}_b\big]. \tag{29}$$

To evaluate the averages in Eq. (23), we consider several approximations. First, we assume that

$$\langle v\sigma_{\rm tr}(k)\mathbf{k}_a \cdot \mathbf{k}_b\rangle_b \simeq 0. \tag{30}$$

This is reasonable since the particle and bath momenta are uncorrelated and the gas is supposed to be at rest: $\langle \mathbf{k}_b\rangle_b = \mathbf{0}$. In the same spirit, we assume that $v\sigma_{\rm tr}(k)$ varies slowly enough around the mass center of the momentum distributions $\rho_a(\mathbf{k}_a)$ and $\rho_b(\mathbf{k}_b)$ to use the approximations

$$\begin{aligned}\big\langle v\sigma_{\rm tr}(k)\mathbf{k}_b^2\big\rangle_b &\simeq \langle v\sigma_{\rm tr}(k)\rangle_b\big\langle\mathbf{k}_b^2\big\rangle_b,\\ \big\langle v\sigma_{\rm tr}(k)\mathbf{k}_a^2\big\rangle_a &\simeq \langle v\sigma_{\rm tr}(k)\rangle_a\big\langle\mathbf{k}_a^2\big\rangle_a.\end{aligned} \tag{31}$$

From Eqs. (23) and (29), a simple closed equation for the mean particle energy is finally obtained

$$\frac{d\big\langle E_{\mathbf{k}_a}\big\rangle}{dt} = 2\eta\big(\big\langle E_{\mathbf{k}_b}\big\rangle - \big\langle E_{\mathbf{k}_a}\big\rangle\big), \tag{32}$$

where η is an energy-based friction coefficient defined as

$$\eta = \frac{m_a m_b}{M^2}\langle nv\sigma_{\rm tr}(k)\rangle. \tag{33}$$

In Eqs. (32) and (33), $\langle\cdot\rangle$ denotes the average over the momenta of both the bath and the particle.

If η is assumed to be time independent, then the solution of Eq. (32) simply reads

$$\big\langle E_{\mathbf{k}_a}(t)\big\rangle = \big[\big\langle E_{\mathbf{k}_a}(0)\big\rangle - \big\langle E_{\mathbf{k}_b}\big\rangle\big]e^{-2\eta t} + \big\langle E_{\mathbf{k}_b}\big\rangle \tag{34}$$

for any initial energy $\langle E_{\mathbf{k}_a}(0)\rangle$ for the particle. The solution (34) implies that the mean particle energy always tends to the mean energy $\langle E_{\mathbf{k}_b}\rangle = \frac{d}{2}k_{\rm B}T$ of the generic bath scatterer, T being the absolute temperature. This result is consistent with the thermalization process whereby the quantum particle reaches thermal equilibrium with the bath.

In the framework of swift charged particles traveling through matter, the governing equation of the mean energy is the famous Bethe formula [32–36]

$$\frac{d\big\langle E_{\mathbf{k}_a}\big\rangle}{dx} = -S\big(\big\langle E_{\mathbf{k}_a}\big\rangle\big), \tag{35}$$

where S denotes the stopping power, which is a known function of the energy, and x is the total path length of the particle. The stopping power mainly accounts for the Coulomb interaction between the swift particle and the electrons of the medium. If the contribution from the thermal bath is neglected in Eq. (32), then Eqs. (32) and (35) are completely analogous, and the energy-dependent friction parameter η can be identified as

$$\eta = \frac{\sqrt{\langle\mathbf{v}_a^2\rangle}}{2\big\langle E_{\mathbf{k}_a}\big\rangle}S\big(\big\langle E_{\mathbf{k}_a}\big\rangle\big), \tag{36}$$

since the path length element is on average given by $dx^2 = \langle\mathbf{v}_a^2\rangle dt^2$. In principle, Eq. (36) can be used to adjust the value of η on experimental measurements of the stopping power [52]. It is remarkable that such an adjustment is feasible, despite the fact that long-range interactions, such as the Coulomb interaction, are beyond the scope of validity of the present model.

The same reasoning based on Eq. (17) can be applied to the mean momentum $\langle\mathbf{k}_a\rangle$. The calculations are very similar to the previous ones and the result reads

$$\frac{d\langle\mathbf{k}_a\rangle}{dt} = -\zeta\langle\mathbf{k}_a\rangle, \tag{37}$$

where ζ is a momentum-based friction coefficient defined as

$$\zeta = \frac{m_b}{M}\langle nv\sigma_{\rm tr}(k)\rangle. \tag{38}$$

Equation (37) shows that, in contrast to the mean energy, the mean momentum tends to zero upon thermalization. Note, in addition, that the characteristic relaxation rate denoted by ζ in Eq. (37) is different from η. The momentum-based parameter is always larger ($\zeta > \eta$), although this difference is negligible for a very heavy particle ($m_a \gg m_b$).

Finally, in the long-time limit ($t \to \infty$), the reduced density matrix of the particle tends to the equilibrium Boltzmann distribution

$$\hat{\rho}_a \propto e^{-\hbar^2\hat{\mathbf{k}}_a^2/2m_a k_{\rm B}T}. \tag{39}$$

This is typically shown by applying the detailed balance condition [45] to Eq. (6). It can also be interpreted as a consequence of the relaxation process described by the Fokker-Planck equation derived in Sec. III.

B. Decoherence in position space

In this section we consider the other important property of the Redfield equation (4), namely, the decoherence. In particular, we seek to know how decoherence affects the density matrix in the position space. To this end, we assume that the density matrix of the particle is initially in the momentum eigenstate at $t = 0$,

$$\hat{\rho}_a(0) = |\mathbf{k}_{a,0}\rangle\langle\mathbf{k}_{a,0}|. \tag{40}$$

In this particular case, $\hat{\rho}_a(t)$ remains diagonal in momentum space due to the gas uniformity, so we have $[\hat{H}_a, \hat{\rho}_a]{=}0\,\forall\, t{>}0$,

and only the dissipator survives in Eq. (4). Under such circumstances, we find in the position representation

$$\frac{\partial \rho_a}{\partial t}(\mathbf{r}, \tilde{\mathbf{r}}, t) = \langle \mathbf{r}|\mathcal{R}_a \hat{\rho}_a(t)|\tilde{\mathbf{r}}\rangle. \tag{41}$$

Expanding the right-hand side of Eq. (41) by means of Eq. (6) leads to

$$\frac{\partial \rho_a}{\partial t}(\mathbf{r}, \tilde{\mathbf{r}}, t) = \sum_{\mathbf{q}} (e^{i\mathbf{q}\cdot(\mathbf{r}-\tilde{\mathbf{r}})} - 1) W_{\mathbf{q}}(\mathbf{k}_{a,0}) \rho_a(\mathbf{r}, \tilde{\mathbf{r}}, t), \tag{42}$$

assuming that, at the beginning of the interaction with the gas, the momentum distribution of the incident particle remains close to the initial one in Eq. (40). Given the structure of Eq. (42), it is useful to introduce what is often called the decoherence rate [12,13,16–18,22,38,43,45,46,53]

$$F(\mathbf{s}) = \sum_{\mathbf{q}} (1 - e^{i\mathbf{q}\cdot\mathbf{s}}) W_{\mathbf{q}}(\mathbf{k}_{a,0}), \tag{43}$$

where $\mathbf{s} = \mathbf{r} - \tilde{\mathbf{r}}$. Equation (43) means that the decoherence rate $F(\mathbf{s})$ is directly given by the Fourier transform of the total collision rate $W_{\mathbf{q}}(\mathbf{k}_{a,0})$. In the continuum limit ($V \to \infty$), Eq. (43) can also be expressed in terms of the differential cross section according to Eq. (12). We get

$$F(\mathbf{s}) = \oint_{\mathcal{S}_d} d\Omega \left\langle nv \frac{d\sigma}{d\Omega}(\mathbf{\Omega}|k\mathbf{\Omega}_0)(1 - e^{ik(\mathbf{\Omega}-\mathbf{\Omega}_0)\cdot\mathbf{s}}) \right\rangle_b, \tag{44}$$

where $\mathbf{k} = k\mathbf{\Omega}_0$ and $\mathbf{v} = v\mathbf{\Omega}_0$ are given by Eqs. (13) and (14), respectively, as usual, but for the special value $\mathbf{k}_a = \mathbf{k}_{a,0}$. Using the denotation $F(\mathbf{s})$, Eq. (42) reads

$$\frac{\partial \rho_a}{\partial t}(\mathbf{r}, \tilde{\mathbf{r}}) = -F(\mathbf{r} - \tilde{\mathbf{r}}) \rho_a(\mathbf{r}, \tilde{\mathbf{r}}) \tag{45}$$

and can be easily integrated as follows:

$$\rho_a(\mathbf{r}, \tilde{\mathbf{r}}, t) = e^{-F(\mathbf{r}-\tilde{\mathbf{r}})t} \rho_a(\mathbf{r}, \tilde{\mathbf{r}}, 0). \tag{46}$$

Since $F(\mathbf{s})$ is complex valued, it is convenient to separate its real and imaginary parts:

$$F(\mathbf{s}) = \mathrm{Re}\, F(\mathbf{s}) + i\, \mathrm{Im}\, F(\mathbf{s}). \tag{47}$$

The real part of $F(\mathbf{s})$ explicitly reads

$$\mathrm{Re}\, F(\mathbf{s}) = \sum_{\mathbf{q}} [1 - \cos(\mathbf{q}\cdot\mathbf{s})] W_{\mathbf{q}}(\mathbf{k}_{a,0}). \tag{48}$$

Since $W_{\mathbf{q}} \geqslant 0$ and $\cos\alpha \leqslant 1$, this function is necessarily positive:

$$\mathrm{Re}\, F(\mathbf{s}) \geqslant 0. \tag{49}$$

Therefore, according to the sign convention in Eqs. (45) and (46), the function $\mathrm{Re}\, F(\mathbf{s})$ represents the exponential decay rate of the off-diagonal entries of $\rho_a(\mathbf{r}, \tilde{\mathbf{r}})$. This decay is the signature of decoherence in position space. In contrast, the imaginary part of $F(\mathbf{s})$, given by

$$\mathrm{Im}\, F(\mathbf{s}) = -\sum_{\mathbf{q}} \sin(\mathbf{q}\cdot\mathbf{s}) W_{\mathbf{q}}(\mathbf{k}_{a,0}), \tag{50}$$

represents the oscillation frequency of the off-diagonal entries. At $\mathbf{r} = \tilde{\mathbf{r}}$, the decoherence rate (43) vanishes [$F(\mathbf{0}) = 0$]. Moreover, at large separation distance ($\|\mathbf{r} - \tilde{\mathbf{r}}\| \to \infty$), it reaches the saturation value [13,16–18,22,38,45,53]

$$F(\mathbf{s}) \xrightarrow{\|\mathbf{s}\|\to\infty} \sum_{\mathbf{q}} W_{\mathbf{q}}(\mathbf{k}_{a,0}) = W_{\mathrm{tot}}(\mathbf{k}_{a,0}), \tag{51}$$

which turns out to be equal to the total collision rate of the particle in the gas: $W_{\mathrm{tot}}(\mathbf{k}_{a,0}) = \langle nv\sigma(k)\rangle_b$. This saturated regime was successfully observed for matter waves in [16,24,25] and previously for light waves [38].

III. KRAMERS-MOYAL APPROXIMATION

In this section approximations of the Redfield equation (4) are established based on the assumption that the deflections undergone by the particle due to the collisions are relatively small. Under this assumption, it is appropriate to expand the first term of the dissipator (6) using the Kramers-Moyal expansion [39–42]. In the quantum-mechanical framework of Eq. (6), this expansion is achieved in practice by

$$e^{i\mathbf{q}\cdot\hat{\mathbf{r}}} \hat{X} e^{-i\mathbf{q}\cdot\hat{\mathbf{r}}} \simeq \hat{X} + iq_i[\hat{r}_i, \hat{X}] + \frac{i^2}{2!} q_i q_j [\hat{r}_i, [\hat{r}_j, \hat{X}]], \tag{52}$$

where $\hat{X}$ stands for $\frac{1}{2}\{\hat{W}_{\mathbf{q}}, \hat{\rho}_a\}$. In Eq. (52) and throughout this section, the implicit summation over the repeated indices $i, j \in \{1, 2, \ldots, d\}$ will be used.

As we will see later, the assumption of small deflections is relevant in two different situations: Either the incident particle is much heavier than the gas particles, that is,

$$m_a \gg m_b, \tag{53}$$

or the differential cross section $\frac{d\sigma}{d\Omega}$ is very peaked in the forward direction ($\mathbf{\Omega} = \mathbf{\Omega}_0$). The latter condition can be formulated by requiring the transfer cross section $\sigma_{\mathrm{tr}}(k)$, defined in Eq. (25), to be much smaller than the total cross section $\sigma(k)$:

$$\sigma_{\mathrm{tr}}(k) \ll \sigma(k). \tag{54}$$

If at least one of the two conditions (53) or (54) is fulfilled, then the expansion (52) is justified. Since they are not mutually exclusive, they can both be satisfied at the same time. This will be the case, for instance, in Sec. IV C when considering an α particle of a few MeVs.

Using Eq. (52) to expand the dissipator (6), we find

$$\mathcal{R}_a \hat{\rho}_a \simeq \frac{i}{2}\left[\hat{r}_i, \left\{\hat{A}_i^{(1)}, \hat{\rho}_a\right\}\right] - \frac{1}{4}\left[\hat{r}_i, \left[\hat{r}_j, \left\{\hat{A}_{ij}^{(2)}, \hat{\rho}_a\right\}\right]\right], \tag{55}$$

where the tensor operators $\hat{A}_i^{(1)}$ and $\hat{A}_{ij}^{(2)}$ are the first and second moments of the total collision rate $\hat{W}_{\mathbf{q}}$, respectively. They are defined as

$$\hat{A}_i^{(1)} = \sum_{\mathbf{q}} q_i W_{\mathbf{q}}(\hat{\mathbf{k}}_a) \tag{56}$$

and

$$\hat{A}_{ij}^{(2)} = \sum_{\mathbf{q}} q_i q_j W_{\mathbf{q}}(\hat{\mathbf{k}}_a). \tag{57}$$

The quantities (56) and (57) will be calculated in detail in Sec. III A. Finally, we assume that the density matrix of the

particle is approximately diagonal in the momentum basis

$$[\hat{\mathbf{k}}_a, \hat{\rho}_a] \simeq \mathbf{0}. \tag{58}$$

This will be the case for sufficiently broad wave packets. As discussed in the previous paper [31], this condition also ensures the complete positivity of the Redfield equation (4). A consequence of Eq. (58) is that the anticommutators in Eq. (55) can be replaced by a simple product

$$\mathcal{R}_a\hat{\rho}_a \simeq i\big[\hat{r}_i, \hat{A}_i^{(1)}\hat{\rho}_a\big] - \tfrac{1}{2}\big[\hat{r}_i, \big[\hat{r}_j, \hat{A}_{ij}^{(2)}\hat{\rho}_a\big]\big]. \tag{59}$$

This approximation will be helpful later in Sec. III B when introducing transverse decoherence.

A. Calculation of the moments

1. First moment

We calculate the first-order moment (56) in vector notation from the property (12),

$$\mathbf{A}^{(1)} = \oint_{\mathcal{S}_d} d\Omega \left\langle nv \frac{d\sigma}{d\Omega}(\mathbf{\Omega}|k\mathbf{\Omega}_0)\mathbf{q} \right\rangle_b. \tag{60}$$

Using Eq. (26), we get, from Eq. (60),

$$\mathbf{A}^{(1)} = -\langle nv\sigma_{\rm tr}(k)\mathbf{k}\rangle_b. \tag{61}$$

This expression can be further simplified using an approximation similar to Eq. (30):

$$\mathbf{A}^{(1)} = -\frac{m_b}{M}\langle nv\sigma_{\rm tr}(k)\rangle_b \mathbf{k}_a. \tag{62}$$

This is all for the first-order moment. Note that the operator nature of $\mathbf{A}^{(1)}$ coming from the momentum $\hat{\mathbf{k}}_a$ should be restored before substituting into Eq. (59).

2. Second moment

Next we consider the second-order moment (57). Using again the property (12), we can write in tensor notation

$$\mathsf{A}^{(2)} = \oint_{\mathcal{S}_d} d\Omega \left\langle nv \frac{d\sigma}{d\Omega}(\mathbf{\Omega}|k\mathbf{\Omega}_0)\mathbf{q}\otimes\mathbf{q} \right\rangle_b, \tag{63}$$

where $\otimes$ denotes the dyadic product, or tensor product, of two vectors. The quantity $\mathsf{A}^{(2)}$ is thus a $d\times d$ matrix. To calculate the tensor in Eq. (63), we decompose the outgoing direction $\mathbf{\Omega}$ into the parallel and perpendicular components to the initial direction of motion $\mathbf{\Omega}_0$. Denoting the unit vector in the transverse direction by $\mathbf{\Omega}_\perp$, we write

$$\mathbf{\Omega} = \cos\theta\, \mathbf{\Omega}_0 + \sin\theta\, \mathbf{\Omega}_\perp, \tag{64}$$

with $\mathbf{\Omega}_0\cdot\mathbf{\Omega}_\perp = 0$ by definition of $\mathbf{\Omega}_\perp$. The integral over $\mathbf{\Omega}$ in Eq. (63) thus splits into two integrals over θ and $\mathbf{\Omega}_\perp$. The differential element of the solid angle in arbitrary dimension $d \geqslant 2$ reads [54]

$$d\Omega = (\sin\theta)^{d-2} d\theta d\Omega_\perp. \tag{65}$$

Knowing that the cross section does not depend on the azimuthal direction $\mathbf{\Omega}_\perp$, we get

$$\mathsf{A}^{(2)} = \left\langle k^2 nv S_{d-1} \int_0^\pi d\theta (\sin\theta)^{d-2} \frac{d\sigma}{d\Omega}(k,\theta)\mathsf{I}(\theta) \right\rangle_b, \tag{66}$$

using the angular tensor

$$\mathsf{I}(\theta) = \oint_{\mathcal{S}_{d-1}} \frac{d\Omega_\perp}{S_{d-1}} [(\cos\theta - 1)\mathbf{\Omega}_0 + \sin\theta\, \mathbf{\Omega}_\perp]^{\otimes 2}, \tag{67}$$

where $\mathbf{a}^{\otimes 2} = \mathbf{a}\otimes\mathbf{a}$ denotes the dyadic square, or tensor square. The tensor (67) can first be simplified due to the fact that the average of $\mathbf{\Omega}_\perp$ is zero. This step removes the cross products of the form $\mathbf{\Omega}_0\otimes\mathbf{\Omega}_\perp$ and leads to

$$\mathsf{I}(\theta) = \oint_{\mathcal{S}_{d-1}} \frac{d\Omega_\perp}{S_{d-1}} (1-\cos\theta)^2 \mathbf{\Omega}_0^{\otimes 2} + \sin^2\theta\, \mathbf{\Omega}_\perp^{\otimes 2}. \tag{68}$$

The first term of Eq. (68) is trivial and the second term is given by

$$\oint_{\mathcal{S}_{d-1}} \frac{d\Omega_\perp}{S_{d-1}} \mathbf{\Omega}_\perp^{\otimes 2} = \frac{\mathsf{1} - \mathbf{\Omega}_0^{\otimes 2}}{d-1}, \tag{69}$$

where $\mathsf{1}$ represents the $d\times d$ identity matrix. The quantity $\mathsf{1} - \mathbf{\Omega}_0^{\otimes 2}$ on the right-hand side of Eq. (69) is the projection matrix on the plane transverse to the direction of motion. Once diagonalized, this matrix is equal to 1 in all the directions perpendicular to $\mathbf{\Omega}_0$ and 0 in the parallel direction. Thus, we arrive at the expression of the angular tensor

$$\mathsf{I}(\theta) = (1-\cos\theta)^2 \mathbf{\Omega}_0^{\otimes 2} + \sin^2\theta \frac{\mathsf{1} - \mathbf{\Omega}_0^{\otimes 2}}{d-1}. \tag{70}$$

When comparing to Eq. (66), the tensor (70) suggests to introduce two quadratic moments related to the cross section, namely,

$$\begin{aligned}\sigma_{\rm q\parallel}(k) &= \oint_{\mathcal{S}_d} d\Omega (1 - \mathbf{\Omega}\cdot\mathbf{\Omega}_0)^2 \frac{d\sigma}{d\Omega}(\mathbf{\Omega}|k\mathbf{\Omega}_0) \\ &= S_{d-1}\int_0^\pi d\theta (\sin\theta)^{d-2}(1-\cos\theta)^2 \frac{d\sigma}{d\Omega}(k,\theta)\end{aligned} \tag{71}$$

for the longitudinal component and

$$\begin{aligned}\sigma_{\rm q\perp}(k) &= \oint_{\mathcal{S}_d} d\Omega [1 - (\mathbf{\Omega}\cdot\mathbf{\Omega}_0)^2] \frac{d\sigma}{d\Omega}(\mathbf{\Omega}|k\mathbf{\Omega}_0) \\ &= S_{d-1}\int_0^\pi d\theta (\sin\theta)^{d-2} \sin^2\theta \frac{d\sigma}{d\Omega}(k,\theta)\end{aligned} \tag{72}$$

for the transverse component. We note that the arithmetic mean of these two quantities is exactly equal to the transfer cross section (25)

$$\frac{\sigma_{\rm q\parallel}(k) + \sigma_{\rm q\perp}(k)}{2} = \sigma_{\rm tr}(k). \tag{73}$$

The expression (73) will be useful to evaluate one of the two quantities when only the other is known. Using the notation in (71) and (72), Eq. (66) reduces to

$$\mathsf{A}^{(2)} = \left\langle k^2 nv \left(\sigma_{\rm q\parallel}(k)\mathbf{\Omega}_0^{\otimes 2} + \sigma_{\rm q\perp}(k)\frac{\mathsf{1} - \mathbf{\Omega}_0^{\otimes 2}}{d-1} \right) \right\rangle_b. \tag{74}$$

In addition, since the incident relative momentum is given by $\mathbf{k} = k\mathbf{\Omega}_0$, Eq. (74) can also be rewritten as

$$\mathsf{A}^{(2)} = \left\langle nv\sigma_{\rm q\parallel}(k)\mathbf{k}^{\otimes 2} + nv\sigma_{\rm q\perp}(k)\frac{k^2\mathsf{1} - \mathbf{k}^{\otimes 2}}{d-1} \right\rangle_b. \tag{75}$$

In order to expand Eq. (75), we assume, as in Sec. II A, that the cross section is a sufficiently smooth function of k to use the approximation

$$\langle v\sigma_\mu(k) f(\mathbf{k})\rangle_b \simeq \langle v\sigma_\mu(k)\rangle_b \langle f(\mathbf{k})\rangle_b, \tag{76}$$

where $\sigma_\mu(k)$ denotes any type of cross-sectional moments, including $\sigma_{\mathrm{q}\parallel}(k)$, $\sigma_{\mathrm{q}\perp}(k)$, or $\sigma_{\mathrm{tr}}(k)$, and $f(\mathbf{k})$ represents any function of $\mathbf{k}$. On the one hand, the assumption (76) allows us to define collisional rates per unit time as

$$\alpha_\mu(k_a) = \langle nv\sigma_\mu(k)\rangle_b. \tag{77}$$

On the other hand, it is possible to evaluate the average of $f(\mathbf{k})$ over the bath in this case. Using Eq. (13), the average of $\mathbf{k}^{\otimes 2}$ reads

$$\langle \mathbf{k}^{\otimes 2}\rangle_b = \frac{m_b^2}{M^2}\mathbf{k}_a^{\otimes 2} + \frac{m_a^2}{M^2}\frac{\langle \mathbf{k}_b^2\rangle_b}{d}\mathsf{1}. \tag{78}$$

The average of the scalar product $\mathbf{k}^2$ is just the trace of the result (78),

$$\langle \mathbf{k}^2\rangle_b = \frac{m_b^2}{M^2}\mathbf{k}_a^2 + \frac{m_a^2}{M^2}\langle \mathbf{k}_b^2\rangle_b. \tag{79}$$

Finally, substituting Eqs. (78) and (79) into Eq. (75) and using Eq. (73) leads to the result

$$\mathsf{A}^{(2)} = \alpha_{\mathrm{q}\parallel}\frac{m_b^2}{M^2}\mathbf{k}_a^{\otimes 2} + \alpha_{\mathrm{q}\perp}\frac{m_b^2}{M^2}\frac{\mathbf{k}_a^2\mathsf{1} - \mathbf{k}_a^{\otimes 2}}{d-1} + 2\alpha_{\mathrm{tr}}\frac{m_a^2}{M^2}k_{\mathrm{T}}^2\mathsf{1}, \tag{80}$$

where k_{T} is a compact denotation for the characteristic wave number of the bath:

$$k_{\mathrm{T}}^2 = \frac{\langle \mathbf{k}_b^2\rangle_b}{d}. \tag{81}$$

In the special case of a classical gas described at equilibrium by the Maxwell-Boltzmann velocity distribution [13,16,17,55], the characteristic wave number is given by

$$k_{\mathrm{T}}^2 = \frac{m_b}{\hbar^2}k_{\mathrm{B}}T. \tag{82}$$

B. Caldeira-Leggett form of the master equation

We return to the expansion (59) of the dissipator in order to substitute the expressions found in Eqs. (62) and (80). It is useful to assume that the collisional rates $\alpha_\mu(k)$ are smooth enough functions of k to get them out of the commutators $[\hat{\mathbf{r}}, \cdot]$. The result is

$$\begin{aligned}\frac{\partial\hat{\rho}_a}{\partial t} - \mathcal{L}_a\hat{\rho}_a = &-i\alpha_{\mathrm{tr}}\frac{m_b}{M}[\hat{r}_i, \hat{k}_{a,i}\hat{\rho}_a]\\ &- \frac{\alpha_{\mathrm{q}\parallel}}{2}\frac{m_b^2}{M^2}[\hat{r}_i, [\hat{r}_j, \hat{k}_{a,i}\hat{k}_{a,j}\hat{\rho}_a]]\\ &- \frac{\alpha_{\mathrm{q}\perp}}{2}\frac{m_b^2}{M^2}\left[\hat{r}_i, \left[\hat{r}_j, \frac{\hat{\mathbf{k}}_a^2\delta_{ij} - \hat{k}_{a,i}\hat{k}_{a,j}}{d-1}\hat{\rho}_a\right]\right]\\ &- \alpha_{\mathrm{tr}}\frac{m_a^2}{M^2}k_{\mathrm{T}}^2[\hat{r}_i, [\hat{r}_i, \hat{\rho}_a]].\end{aligned} \tag{83}$$

This equation has a form similar to the Caldeira-Leggett master equation [16,17,43–46]. As a reminder, the Caldeira-Leggett equation was derived for a different model in which the particle is coupled to a thermal bath of harmonic oscillators. In fact, Eq. (83) reduces to the usual Caldeira-Leggett equation in the limit $m_a \gg m_b$ for the Brownian motion, because the terms with the coefficients $\alpha_{\mathrm{q}\parallel}$ and $\alpha_{\mathrm{q}\perp}$ are then negligible.

The first term on the right-hand side of Eq. (83) can be interpreted as friction, the second term as decoherence parallel to the direction of motion, and the third term as decoherence in the transverse direction. The last term is the additional contribution to decoherence due to the thermal motion of the scatterers. This contribution is isotropic since it acts equally in all directions.

One can check that the evolution equations of the moments $\langle E_{\mathbf{k}_a}\rangle$ and $\langle \mathbf{k}_a\rangle$ predicted by Eq. (83) indeed reduce to Eqs. (32) and (37) obtained in Sec. II A. In particular, all the terms of Eq. (83) contribute to the evolution of $\langle E_{\mathbf{k}_a}\rangle$, but only the first one, namely, the friction term, contributes to the evolution of $\langle \mathbf{k}_a\rangle$.

1. *Strongly forward scattering*

Here we simplify Eq. (83) by accounting for the strong directionality of the cross section in the forward direction. This directionality is especially expected for high-energy particles. The assumption of strong forward scattering typically implies that the transfer cross section is much smaller than the total cross section, as in Eq. (54). Under this assumption, the moments of the cross section defined in Eqs. (71) and (72) can be approximated as

$$\begin{aligned}\sigma_{\mathrm{q}\parallel}(k) &= \sigma(k)\langle(1-\cos\theta)^2\rangle \simeq \tfrac{1}{4}\sigma(k)\langle\theta^4\rangle,\\ \sigma_{\mathrm{q}\perp}(k) &= \sigma(k)\langle\sin^2\theta\rangle \simeq \sigma(k)\langle\theta^2\rangle,\end{aligned} \tag{84}$$

where $\langle\cdot\rangle$ denotes the average weighted by the differential cross section $\frac{d\sigma}{d\Omega}$. Indeed, the scattering angle θ is relatively small compared to 1. The fourth angular moment can be related to the kurtosis κ as $\langle\theta^4\rangle = \kappa\langle\theta^2\rangle^2$. If the differential cross section is mesokurtic, i.e., similar to a normal distribution, then we have $\kappa = 3$. Moreover, since it is known that the transfer cross section is approximately $\sigma_{\mathrm{tr}}(k) \simeq \frac{1}{2}\sigma(k)\langle\theta^2\rangle$, we can write

$$\begin{aligned}\sigma_{\mathrm{q}\parallel}(k) &\simeq \kappa\frac{\sigma_{\mathrm{tr}}(k)^2}{\sigma(k)} \ll \kappa\sigma_{\mathrm{tr}}(k),\\ \sigma_{\mathrm{q}\perp}(k) &\simeq 2\sigma_{\mathrm{tr}}(k).\end{aligned} \tag{85}$$

If κ is of the order of 3, then Eq. (85) shows that the longitudinal moment is typically much smaller than the transverse moment $[\sigma_{\mathrm{q}\parallel}(k) \ll \sigma_{\mathrm{q}\perp}(k)]$ and can be neglected. Therefore, reasonable values for the cross-sectional moments (85) could be

$$\sigma_{\mathrm{q}\parallel}(k) \simeq 0, \quad \sigma_{\mathrm{q}\perp}(k) \simeq 2\sigma_{\mathrm{tr}}(k). \tag{86}$$

In this way, the moments still satisfy the constraint given by Eq. (73). Note that assuming $\sigma_{\mathrm{q}\parallel}(k) \simeq 0$ completely discards the longitudinal momentum diffusion. This can be geometrically understood from Fig. 1. Indeed, when $|\tilde{u}(\mathbf{q})|^2$ is concentrated at $\mathbf{q} = \mathbf{0}$, the outgoing momenta are constrained to a very thin region which mostly extends in the transverse directions. Accordingly, the momentum diffuses much more slowly in the longitudinal direction.

Letting $\alpha_{q\parallel}$ tend to zero in Eq. (83) leads to

$$\frac{\partial\,\hat\rho_a}{\partial t} - \mathcal{L}_a\hat\rho_a = -i\alpha_{\rm tr}\frac{m_b}{M}[\hat r_i, \hat k_{a,i}\hat\rho_a] - \alpha_{\rm tr}\frac{m_b^2}{M^2}\left[\hat r_i, \left[\hat r_j, \frac{\hat{\mathbf{k}}_a^2\delta_{ij} - \hat k_{a,i}\hat k_{a,j}}{d-1}\hat\rho_a\right]\right] - \alpha_{\rm tr}\frac{m_a^2}{M^2}k_{\rm T}^2[\hat r_i, [\hat r_i, \hat\rho_a]]. \quad (87)$$

Let us focus on the second term of Eq. (87) associated with the deflection of the particle in the directions perpendicular to the direction of motion. To better understand this term, it is useful to express it in terms of the angular momentum operator, which is defined in arbitrary dimension as

$$\hat L_{ij} = \hat r_i\hat k_{a,j} - \hat r_j\hat k_{a,i}. \quad (88)$$

The operator $\hat L_{ij}$ is the generator of the rotation in the plane ij and thus acts in both position and momentum spaces.

The second term of Eq. (87) can be related to $\hat L_{ij}$ by the nontrivial property

$$\left[\hat r_i, \left[\hat r_j, \left(\hat{\mathbf{k}}_a^2\delta_{ij} - \hat k_{a,i}\hat k_{a,j}\right)\hat\rho_a\right]\right] = \tfrac{1}{2}[\hat L_{ij}, [\hat L_{ij}, \hat\rho_a]] - i(d-1)[\hat r_i, \hat k_{a,i}\hat\rho_a], \quad (89)$$

which is proved in the Appendix under the approximation (58). The interest of Eq. (89) is the separation of the purely transverse contribution to decoherence (the first term on the right-hand side) from the residual contribution to the mean energy (the second term). Substituting Eq. (89) into Eq. (87) yields

$$\frac{\partial\,\hat\rho_a}{\partial t} - \mathcal{L}_a\hat\rho_a = -i\alpha_{\rm tr}\frac{m_am_b}{M^2}[\hat r_i, \hat k_{a,i}\hat\rho_a] - \frac{\alpha_{\rm tr}}{2}\frac{m_b^2}{M^2}\frac{1}{d-1}[\hat L_{ij}, [\hat L_{ij}, \hat\rho_a]] - \alpha_{\rm tr}\frac{m_a^2}{M^2}k_{\rm T}^2[\hat r_i, [\hat r_i, \hat\rho_a]]. \quad (90)$$

The first and third terms on the right-hand side of Eq. (90) are the friction and decoherence terms, respectively, which are well known in the Caldeira-Leggett master equation [16,17,43–46]. However, the second term represents an additional contribution to the transverse decoherence, which is the central result of this paper. This term has the effect of rotating the wave packet by an infinitesimal angle in a random direction under the impact of collisions with the scatterers.

Furthermore, we note that the transport parameters in Eq. (90) merely depend on the transfer cross section (25). The transfer cross section is thus the main relevant phenomenological parameter governing the transport of fast particles in matter [56].

2. *Wigner representation*

In this section the Wigner transform of Eq. (90) is derived. As a reminder, the Wigner transform can be defined in either the position or the momentum basis as [57–60]

$$\mathcal{W}(\hat A) = \int_{\mathbb{R}^d}\frac{d\mathbf{s}}{(2\pi)^d}\left\langle\mathbf{k}_a + \frac{\mathbf{s}}{2}\middle|\hat A\middle|\mathbf{k}_a - \frac{\mathbf{s}}{2}\right\rangle e^{i\mathbf{s}\cdot\mathbf{r}} = \int_{\mathbb{R}^d}\frac{d\mathbf{s}}{(2\pi)^d}\left\langle\mathbf{r} + \frac{\mathbf{s}}{2}\middle|\hat A\middle|\mathbf{r} - \frac{\mathbf{s}}{2}\right\rangle e^{-i\mathbf{k}_a\cdot\mathbf{s}}. \quad (91)$$

In particular, the Wigner transform of the density matrix gives the Wigner function

$$f_a(\mathbf{r}, \mathbf{k}_a) = \mathcal{W}(\hat\rho_a). \quad (92)$$

The function $f_a(\mathbf{r}, \mathbf{k}_a)$ is a real function of the position $\mathbf{r}$ and the momentum $\mathbf{k}_a$. This function is also referred to as a quasiprobability distribution because of its similarity to the classical phase-space distribution. In particular, it is normalized according to[1]

$$\int_{\mathcal{V}} d\mathbf{r}\int_{\mathbb{R}^d} d\mathbf{k}_a f_a(\mathbf{r}, \mathbf{k}_a) = 1. \quad (93)$$

However, in contrast to a usual probability distribution, $f_a(\mathbf{r}, \mathbf{k}_a)$ may be negative, typically in the presence of quantum interferences. Before applying the Wigner transform to Eq. (90), it is useful to consider the following transform of the commutators:

$$\mathcal{W}([\hat{\mathbf{r}}, \hat\rho_a]) = i\boldsymbol{\nabla}_{\mathbf{k}_a}f_a(\mathbf{r}, \mathbf{k}_a),$$
$$\mathcal{W}([\hat{\mathbf{k}}_a, \hat\rho_a]) = -i\boldsymbol{\nabla}_{\mathbf{r}}f_a(\mathbf{r}, \mathbf{k}_a). \quad (94)$$

More generally, each commutator $[\hat{\mathbf{r}}, \cdot]$ or $[\hat{\mathbf{k}}_a, \cdot]$ corresponds to a multiplication by a gradient $i\boldsymbol{\nabla}_{\mathbf{k}_a}$ or $-i\boldsymbol{\nabla}_{\mathbf{r}}$, respectively, in the Wigner representation. In addition, the Wigner transform of the double commutator with $\hat L_{ij}$ is given by

$$\mathcal{W}\left(\tfrac{1}{2}[\hat L_{ij}, [\hat L_{ij}, \hat\rho_a]]\right) = -\nabla^2_{\perp\mathbf{k}_a}f_a(\mathbf{r}, \mathbf{k}_a), \quad (95)$$

where $\nabla^2_{\perp\mathbf{k}_a}$ is the Laplace-Beltrami operator on the spherical submanifold of $\mathbb{R}^d$. The result (95) is proved at the end of the Appendix. Using Eqs. (94) and (95), the Wigner representation of Eq. (90) reads

$$\frac{\partial f_a}{\partial t} + \mathbf{v}_a\cdot\boldsymbol{\nabla}_{\mathbf{r}}f_a = \eta\boldsymbol{\nabla}_{\mathbf{k}_a}\cdot(\mathbf{k}_af_a) + \gamma\nabla^2_{\perp\mathbf{k}_a}f_a + \xi\nabla^2_{\mathbf{k}_a}f_a, \quad (96)$$

where $\mathbf{v}_a = \frac{\hbar\mathbf{k}_a}{m_a}$ is the particle velocity, $\nabla^2_{\mathbf{k}_a}$ denotes the standard Laplace operator, and the transport coefficients are defined as

$$\eta = \frac{m_am_b}{M^2}\alpha_{\rm tr}, \quad \gamma = \frac{m_b^2}{M^2}\frac{\alpha_{\rm tr}}{d-1}, \quad \xi = \frac{m_a^2}{M^2}\alpha_{\rm tr}k_{\rm T}^2. \quad (97)$$

The parameter γ will be referred to as the directional diffusivity, or the transverse diffusivity, and ξ as the momentum diffusivity induced by the bath. It is remarkable that all the parameters in Eq. (97) are determined by the single collisional parameter $\alpha_{\rm tr}$. Between η and ξ, this relationship can be interpreted as a consequence of the fluctuation-dissipation theorem

[1]The position integral is restricted to the region $\mathcal{V}$, because of the periodic boundary conditions on the particle wave function (see also Sec. II).

[45,55]

$$\frac{\xi}{\eta} = \frac{m_a k_B T}{\hbar^2}, \tag{98}$$

assuming k_T is given by Eq. (82).

Equations of the form of Eq. (96) are generally called Fokker-Planck equations [17,43,45,61] or occasionally Kramers equations [46]. Equations similar to Eq. (96) were found in Refs. [37,38] for light beams in the paraxial approximation, but without the friction term.

Finally, it is worth noting that in the context of fast particles which are much faster than the scatterers ($\langle \mathbf{v}_a^2 \rangle \gg \langle \mathbf{v}_b^2 \rangle$), the contribution to the angular diffusion from the term $\xi \nabla_{\mathbf{k}_a}^2 f_a$ can be neglected at the beginning of the propagation.

IV. COHERENCE LENGTH

When studying decoherence on a given density matrix, it can be useful to determine the characteristic length beyond which quantum coherence disappears. This coherence manifests off the diagonal of the density matrix $\rho_a(\mathbf{r}, \tilde{\mathbf{r}})$, that is, for $\mathbf{r} \neq \tilde{\mathbf{r}}$. In practice, the spatial extent of this coherent region can be estimated by the variance of $|\rho_a(\mathbf{r}, \tilde{\mathbf{r}})|^2$ in the separation variable $\mathbf{s} = \mathbf{r} - \tilde{\mathbf{r}}$, as proposed in Ref. [47]. Furthermore, it is also possible to characterize the ellipsoidal shape of the coherent region using the covariance matrix. This idea leads to the definition of the coherence length matrix

$$\Lambda^2 = \frac{\iint_{\mathcal{V}^2} (\mathbf{r} - \tilde{\mathbf{r}})^{\otimes 2} |\rho_a(\mathbf{r}, \tilde{\mathbf{r}})|^2 d\mathbf{r}\, d\tilde{\mathbf{r}}}{2 \iint_{\mathcal{V}^2} |\rho_a(\mathbf{r}, \tilde{\mathbf{r}})|^2 d\mathbf{r}\, d\tilde{\mathbf{r}}}. \tag{99}$$

The factor of 2 in the denominator of Eq. (99) is needed to make this definition consistent with the variance of a pure state $\rho_a(\mathbf{r}, \tilde{\mathbf{r}}) = \psi(\mathbf{r})\psi^*(\tilde{\mathbf{r}})$, as pointed out in Ref. [47]. The definition (99) can also be written using the quantum operator notation as

$$[\Lambda^2]_{ij} = \frac{\mathrm{Tr}_a\left(\hat{\rho}_a^2 \hat{r}_i \hat{r}_j - \hat{\rho}_a \hat{r}_i \hat{\rho}_a \hat{r}_j\right)}{\mathrm{Tr}_a\left(\hat{\rho}_a^2\right)}, \tag{100}$$

but also as

$$[\Lambda^2]_{ij} = -\frac{\mathrm{Tr}_a([\hat{r}_i, \hat{\rho}_a][\hat{r}_j, \hat{\rho}_a])}{2\mathrm{Tr}_a\left(\hat{\rho}_a^2\right)}, \tag{101}$$

or even, using the property $\mathrm{Tr}([\hat{A}, \hat{B}]\hat{C}) = -\mathrm{Tr}(\hat{B}[\hat{A}, \hat{C}])$, as

$$[\Lambda^2]_{ij} = \frac{\mathrm{Tr}_a(\hat{\rho}_a[\hat{r}_i, [\hat{r}_j, \hat{\rho}_a]])}{2\mathrm{Tr}_a\left(\hat{\rho}_a^2\right)}. \tag{102}$$

In addition, the coherence length is related to the Wigner function of the particle by

$$\Lambda^2 = \frac{\iint \nabla_{\mathbf{k}_a} f_a(\mathbf{r}, \mathbf{k}_a) \otimes \nabla_{\mathbf{k}_a} f_a(\mathbf{r}, \mathbf{k}_a) d\mathbf{r}\, d\mathbf{k}_a}{2 \iint f_a(\mathbf{r}, \mathbf{k}_a)^2 d\mathbf{r}\, d\mathbf{k}_a}. \tag{103}$$

The expression (103) comes directly from Eq. (101) using Eq. (94) and the fact that

$$\mathrm{Tr}\left(\hat{\rho}_a^2\right) = (2\pi)^d \iint f_a(\mathbf{r}, \mathbf{k}_a)^2 d\mathbf{r}\, d\mathbf{k}_a. \tag{104}$$

There is yet another form for the coherence length in terms of the Hessian matrix of the Wigner function, which is written

$$\Lambda^2 = -\frac{\iint f_a(\mathbf{r}, \mathbf{k}_a) \nabla_{\mathbf{k}_a} \otimes \nabla_{\mathbf{k}_a} f_a(\mathbf{r}, \mathbf{k}_a) d\mathbf{r}\, d\mathbf{k}_a}{2 \iint f_a(\mathbf{r}, \mathbf{k}_a)^2 d\mathbf{r}\, d\mathbf{k}_a}. \tag{105}$$

This expression can be obtained from the integration by part of Eq. (103) or by analogy from Eq. (102).

Expressions (103) and (105) show that the coherence length is larger when the Wigner function $f_a(\mathbf{r}, \mathbf{k}_a)$ strongly varies in momentum space. In particular, for a very peaked distribution such as for a plane wave, the coherence length can be infinite. Note that the coherence length is also infinite for any discrete superposition of plane waves. As the momentum diffusion takes place, due to the last two terms on the right-hand side of Eq. (96), the momentum distribution smooths out on the continuum and its gradient diminishes. Accordingly, the coherence length Λ^2 is expected to decrease in time.

Furthermore, it should be noted that the definition (99) implicitly assumes that the integral converges. This is not obvious, because the density matrix element given by Eq. (46) in the general case does not vanish to zero for $\|\mathbf{r} - \tilde{\mathbf{r}}\| \to \infty$ but instead tends to a finite value. This is due to the saturation of the decoherence rate observed in Eq. (51). In that case, the coherence length defined as Eq. (99) would be infinite. In fact, this issue is circumvented by the Kramers-Moyal expansion performed in Sec. III, because then the decoherence rate $F(\mathbf{r} - \tilde{\mathbf{r}})$ increases quadratically for $\|\mathbf{r} - \tilde{\mathbf{r}}\| \to \infty$ without any upper bound. In this case, the density matrix element (46) tends to zero for $\|\mathbf{r} - \tilde{\mathbf{r}}\| \to \infty$ and the coherence length is well defined. Therefore, regarding the calculation of the coherence length from Eq. (99), the Kramers-Moyal expansion amounts to neglecting the nonzero asymptotic value of $\rho_a(\mathbf{r}, \tilde{\mathbf{r}})$ for $\|\mathbf{r} - \tilde{\mathbf{r}}\| \to \infty$.

A. Relation to the momentum variance

The distribution predicted by the Fokker-Planck equation (96) in the momentum space is typically of Gaussian nature, as will be seen later in more detail. This is a fundamental feature of diffusion equations and can be interpreted, in the context of random processes, as a consequence of the central limit theorem. An important consequence of this Gaussian profile is that the coherence length turns out to be directly related to the variance of the momentum, as shown in this section. First, we assume that the Wigner function has the form of a multivariate Gaussian distribution

$$f_a(\mathbf{r}, \mathbf{k}_a) = \frac{1}{V(2\pi)^{d/2} \det \mathsf{K}} e^{-(\Delta \mathbf{k}_a)^\intercal \cdot \mathsf{K}^{-2} \cdot \Delta \mathbf{k}_a / 2}, \tag{106}$$

where $\Delta \mathbf{k}_a = \mathbf{k}_a - \langle \mathbf{k}_a \rangle$ is the centered momentum and K^2 is the momentum covariance matrix. The distribution (106) reduces to the equilibrium distribution for $\langle \mathbf{k}_a \rangle = \mathbf{0}$ and $\mathsf{K}^2 = \frac{m_a}{\hbar^2} k_B T \mathsf{1}$. The distribution (106) is normalized according to Eq. (93) and its covariance matrix is given by

$$\int_{\mathcal{V}} d\mathbf{r} \int_{\mathbb{R}^d} d\mathbf{k}_a (\Delta \mathbf{k}_a)^{\otimes 2} f_a(\mathbf{r}, \mathbf{k}_a) = \mathsf{K}^2. \tag{107}$$

Using the gradient of f_a with respect to the momentum

$$\nabla_{\mathbf{k}_a} f_a = -\mathsf{K}^{-2} \cdot \Delta \mathbf{k}_a f_a, \tag{108}$$

the integral in the numerator of Eq. (103) becomes

$$\int \nabla_{\mathbf{k}_a} f_a \otimes \nabla_{\mathbf{k}_a} f_a d\mathbf{k}_a = \int \mathsf{K}^{-2} \cdot (\Delta\mathbf{k}_a)^{\otimes 2} \cdot \mathsf{K}^{-2} f_a^2 d\mathbf{k}_a. \tag{109}$$

The right-hand side of Eq. (109) can be simplified with the property

$$\int (\Delta\mathbf{k}_a)^{\otimes 2} f_a^2 d\mathbf{k}_a = \frac{\mathsf{K}^2}{2} \int f_a^2 d\mathbf{k}_a, \tag{110}$$

which results from the fact that the variance of f_a^2 is half the variance of f_a according to Eq. (106). Therefore, substituting Eq. (110) into Eq. (109) and dividing both sides by $2\int f_a^2 d\mathbf{k}_a$ leads to

$$\Lambda^2 = \frac{\int \nabla_{\mathbf{k}_a} f_a \otimes \nabla_{\mathbf{k}_a} f_a d\mathbf{k}_a}{2\int f_a^2 d\mathbf{k}_a} = \frac{\mathsf{K}^{-2}}{4}, \tag{111}$$

or in simpler terms

$$\Lambda^2 \cdot \mathsf{K}^2 = \frac{1}{4}. \tag{112}$$

The result (112) can also be expressed with the rescaled momentum covariance matrix $\mathsf{P}^2 = \hbar^2\mathsf{K}^2$ as

$$\Lambda^2 \cdot \mathsf{P}^2 = \frac{\hbar^2}{4}\mathsf{1}. \tag{113}$$

Expressions (112) and (113) show that, for Gaussian states, the coherence length can be directly deduced from the knowledge of the momentum variance. In addition, they confirm that the shorter the spatial coherence length, the larger the momentum variance. This duality between position and momentum is strongly reminiscent of Heisenberg's uncertainty principle [59,62–64] for the given direction i,

$$\langle \Delta\hat{r}_i^2 \rangle \langle \Delta\hat{p}_i^2 \rangle \geqslant \frac{\hbar^2}{4}, \tag{114}$$

where $\Delta\hat{r}_i = \hat{r}_i - \langle \hat{r}_i \rangle$ and $\Delta\hat{p}_i = \hat{p}_i - \langle \hat{p}_i \rangle$ are the centered position and momentum, respectively.

The existence of an uncertainty relation for the coherence length follows from the fact that, according to the definition (91), the coherence function $\rho_a(\mathbf{r} + \frac{\mathbf{s}}{2}, \mathbf{r} - \frac{\mathbf{s}}{2})$ of variable $\mathbf{s}$ is related to the Wigner function $f_a(\mathbf{r}, \mathbf{k}_a)$ by the Fourier transform with respect to $\mathbf{s}$, in the same way the position-space and the momentum-space wave functions are related in quantum mechanics. Therefore, Eq. (113) could be generalized to an inequality for non-Gaussian states. However, such a generalization is not needed in this paper because the state will be assumed to be Gaussian. In this context, the strict equality (113) at the lower bound of Eq. (114) implies that the decoherence process in particle detectors could in principle resolve the position of the particle at the quantum limit for an ideal measurement [65].

B. Evolution of the momentum distribution

In view of obtaining approximate expressions for the coherence lengths in the longitudinal and transverse directions, the property (112) will be exploited on estimates for the momentum variances, starting from the initial condition (40), and assuming the transport parameters (97) do not depend on the particle energy. In this way, finding the explicit solution of the Fokker-Planck equation (96) is not necessary. The interest of this approach is that the momentum variance, defined as

$$K^2 = \mathrm{Tr}(\mathsf{K}^2) = \mathrm{Var}(\mathbf{k}_a) = \langle \mathbf{k}_a^2 \rangle - \langle \mathbf{k}_a \rangle^2, \tag{115}$$

can be found from the moment equations (32) and (37) derived in the general case, hence bypassing Eq. (96). This approach should nevertheless lead to results consistent with Eq. (96). The equation for the average momentum is the same as Eq. (37), repeated here for convenience: $\frac{d\langle \mathbf{k}_a \rangle}{dt} = -\zeta \langle \mathbf{k}_a \rangle$. The solution to Eq. (37), subjected to the initial condition $\langle \mathbf{k}_a(0) \rangle = \mathbf{k}_{a,0}$, reads

$$\langle \mathbf{k}_a \rangle = \mathbf{k}_{a,0} e^{-\zeta t}. \tag{116}$$

Since the wave number is related to the velocity by $\mathbf{v}_a = \frac{\hbar \mathbf{k}_a}{m_a}$, Eq. (116) leads, after time integration, to the average distance traveled by the particle in its initial direction

$$L_a = \frac{v_{a,0}}{\zeta}(1 - e^{-\zeta t}), \tag{117}$$

where $v_{a,0}$ is the initial velocity of the particle. The total distance traveled by the particle, or range [32–36], is thus $L_{a,\infty} = v_{a,0}/\zeta$. For instance, the well-known range of an α particle of initial kinetic energy of 5 MeV in dry air under normal conditions (20 °C and 1 atm) is $L_{a,\infty} = 3.5$ cm [33,35,36,52,66–68].

It should be noted that, according to the definition (38), ζ can be related to the parameters (97) as

$$\zeta = \frac{m_b}{M}\alpha_{\mathrm{tr}} = \eta + (d-1)\gamma. \tag{118}$$

Equation (118) shows that ζ is related to the directional diffusivity γ, which is not obvious for a friction parameter. This is due to the fact that the directional diffusion, which is described by the γ term in Eq. (96), geometrically contributes to enhance the relaxation of $\langle \mathbf{k}_a \rangle$ in time. When the incident particle is heavy ($m_a \gg m_b$), the parameter γ is much smaller than ζ or η. In this particular case, the parameters ζ and η are approximately equal to each other.

Next to the average momentum, the equation for $\langle \mathbf{k}_a^2 \rangle$ is given by Eq. (32), rewritten here as

$$\frac{d\langle \mathbf{k}_a^2 \rangle}{dt} = -2\eta \langle \mathbf{k}_a^2 \rangle + 2d\xi, \tag{119}$$

using the parameters (97). The solution of Eq. (119) reads, as in Eq. (34),

$$\langle \mathbf{k}_a^2 \rangle = \left(k_{a,0}^2 - \frac{d\xi}{\eta}\right) e^{-2\eta t} + \frac{d\xi}{\eta}. \tag{120}$$

Note that, in Eq. (120), the initial condition $\mathrm{Var}(\mathbf{k}_a) = 0$ and thus $\langle \mathbf{k}_a^2 \rangle = k_{a,0}^2$ was used. This results from the assumption that the initial state is a plane wave. Combining Eqs. (116) and (120) into Eq. (115) leads to

$$K^2 = k_{a,0}^2 (e^{-2\eta t} - e^{-2\zeta t}) + \frac{d\xi}{\eta}(1 - e^{-2\eta t}). \tag{121}$$

This result should be understood as the total variance of the momentum, which is the sum of the longitudinal and the transverse variances. Since there is one longitudinal direction

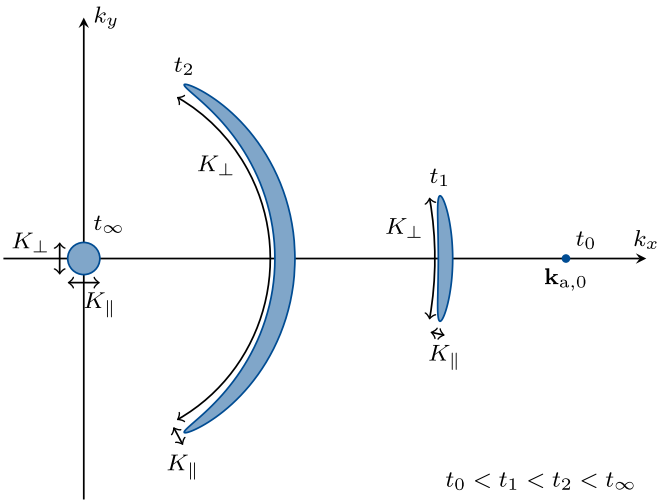

FIG. 2. Schematic representation of the momentum distribution predicted by Eq. (96) at different times. The geometric interpretation of the standard deviations $K_\parallel$ and $K_\perp$ given by Eq. (123) is also highlighted. The time $t_0 = 0$ corresponds to the initial condition and t_∞ to the equilibrium distribution.

and $d-1$ transverse directions in $\mathbb{R}^d$, the total variance (121) can be decomposed as

$$K^2 = K_\parallel^2 + (d-1)K_\perp^2. \tag{122}$$

In order to identify $K_\parallel$ and $K_\perp$ in Eq. (121), one way is to temporarily remove the contribution from the transverse diffusion by letting $\gamma = 0$. Doing so, the parameters ζ and η become equal to each other according to Eq. (118) and the first term on the right-hand side of Eq. (121) vanishes. What remains should correspond to the isotropic contribution from the thermal bath and what disappears should correspond to the contribution to the transverse variance. Therefore, the sought decomposition reads

$$\begin{aligned} K_\parallel^2 &= \frac{\xi}{\eta}(1 - e^{-2\eta t}), \\ K_\perp^2 &= k_{a,0}^2 \frac{e^{-2\eta t} - e^{-2\zeta t}}{d-1} + \frac{\xi}{\eta}(1 - e^{-2\eta t}). \end{aligned} \tag{123}$$

This result can be confirmed by more detailed calculations based on Eq. (96), which are not presented here.

The behavior of the momentum distribution satisfying Eq. (96) is schematically depicted over time in Fig. 2 for the initial momentum $\mathbf{k}_{a,0}$ at time $t_0 = 0$. This figure helps to geometrically interpret the parameters $K_\parallel$ and $K_\perp$ given by Eq. (123). At time t_1, the distribution spreads more in the transverse direction than in the longitudinal direction under the effect of the γ term in Eq. (96). The average momentum $\langle \mathbf{k}_a \rangle$ also gets smaller due to friction. At the later time t_2, the angular aperture of the distribution increases until it forms a spherical cap around the point $\mathbf{k}_a = \mathbf{0}$. At time t_∞ after a while ($t_\infty \to \infty$), the distribution tends to the equilibrium Boltzmann distribution, which is isotropic and centered at $\mathbf{k}_a = \mathbf{0}$.

The behavior depicted in Fig. 2 and in particular the fact that $K_\perp$ increases faster than $K_\parallel$ can be checked in the short-time limit

$$K_\parallel^2 \xrightarrow{t\to 0} 2\xi t, \quad K_\perp^2 \xrightarrow{t\to 0} 2k_{a,0}^2 \gamma t + 2\xi t. \tag{124}$$

In the second of Eqs. (124), we note that the contribution of the term $k_{a,0}^2\gamma$ is much larger than that of ξ for a fast particle ($v_{a,0}^2 \gg \langle \mathbf{v}_b^2 \rangle$). Indeed, the ratio of these parameters reads

$$\frac{k_{a,0}^2 \gamma}{\xi} = \frac{d}{d-1} \frac{v_{a,0}^2}{\langle \mathbf{v}_b^2 \rangle}, \tag{125}$$

according to Eqs. (81) and (97). Furthermore, the two variances in Eq. (123) effectively converge to the same value in the long-time limit:

$$K_\parallel^2 \xrightarrow{t\to\infty} K_\perp^2 \xrightarrow{t\to\infty} \frac{\xi}{\eta} = \frac{m_a}{\hbar^2} k_B T. \tag{126}$$

This is consistent with the regime of thermal equilibrium with the gas shown at time t_∞ in Fig. 2. Indeed, in this regime, the momentum distribution of the particle tends to the Boltzmann distribution (39), which exhibits the same variance in every individual direction and whose value coincides with Eq. (126).

C. Evolution of the coherence lengths

According to the property (112), the result (123) leads to interesting approximations of the coherence lengths in the longitudinal and transverse directions:

$$\Lambda_\parallel = \frac{1}{2K_\parallel}, \quad \Lambda_\perp = \frac{1}{2K_\perp}. \tag{127}$$

The time evolution of the coherence lengths (127) following Eq. (123) is shown in Fig. 3(a) along with the traveled distance (117) in Fig. 3(b). Since $K_\parallel < K_\perp$ in Eq. (123), the coherence length in Eq. (127) is typically smaller in the transverse direction than in the longitudinal direction ($\Lambda_\perp < \Lambda_\parallel$). Therefore, the coherent wave packet can be thought of as an ellipsoid elongated in the direction of motion. According to Eq. (124), the coherence lengths (127) both behave in the short-time limit as the power law $t^{-1/2}$:

$$\begin{aligned} \Lambda_\parallel &\xrightarrow{t\to 0} \tfrac{1}{2}(2\xi t)^{-1/2}, \\ \Lambda_\perp &\xrightarrow{t\to 0} \tfrac{1}{2}\left(2k_{a,0}^2\gamma t + 2\xi t\right)^{-1/2}. \end{aligned} \tag{128}$$

This explains why, in log-log scale, the curves of $\Lambda_\parallel$ and $\Lambda_\perp$ look parallel in Fig. 3(a) for $\eta t \ll 1$. An important consequence is that, at short times, the ratio of the coherence lengths keeps the constant value

$$\frac{\Lambda_\parallel}{\Lambda_\perp} \xrightarrow{t\to 0} \sqrt{1 + \frac{d}{d-1}\frac{v_{a,0}^2}{\langle \mathbf{v}_b^2 \rangle}}, \tag{129}$$

which only depends on the velocities of the incident particle and the scatterers and not on any of the transport parameters that were introduced in Eq. (97). This gives to Eq. (129) a universal nature. Note, however, that Eq. (129) neglects the contribution to longitudinal decoherence of the second term on the right-hand side of Eq. (83). This additional contribution could make the ratio (129) smaller.

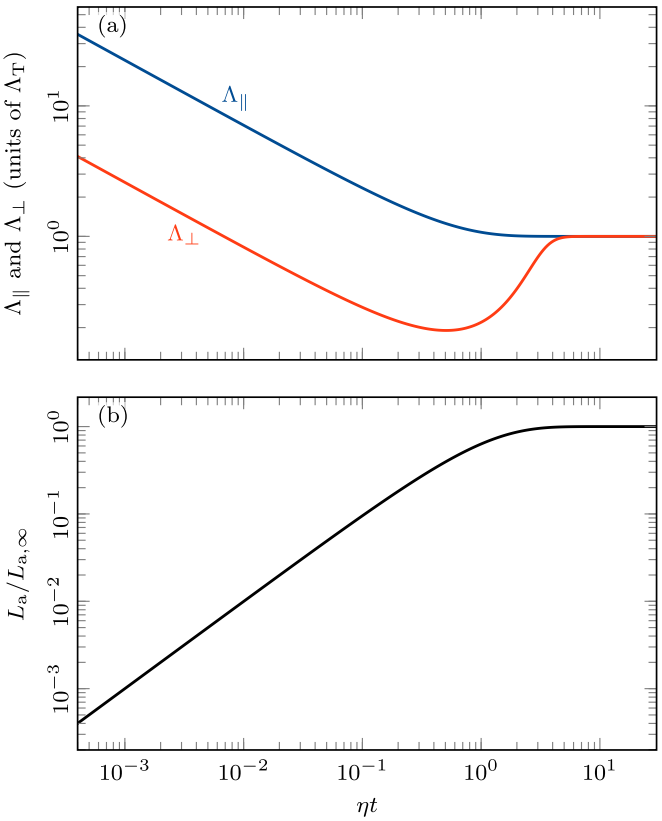

FIG. 3. (a) Coherence lengths $\Lambda_\parallel$ and $\Lambda_\perp$ of the incident particle given by Eqs. (123) and (127) normalized by the equilibrium value Λ_T in Eq. (133). (b) Traveled distance in Eq. (117) as a function of time. The velocity ratio is set to $v_{a,0}/\langle \mathbf{v}_b^2\rangle^{1/2} = 7$ in accordance with Eqs. (130) and (131) and the mass ratio is $m_a/m_b = 10^3$. The curves of both panels depend little on the mass ratio for $m_a \gg m_b$.

Using Eq. (129), the coherence length ratio can be estimated for an α particle of initial kinetic energy of $E_{a,0} = 5$ MeV as considered by Darwin and Mott [1,2]. This particular energy is the most common energy for an α particle generated by natural radioactive emitters such as ^{238}U ($E_\alpha = 4.270$ MeV) [69], ^{226}Ra ($E_\alpha = 4.871$ MeV), ^{222}Rn ($E_\alpha = 5.590$ MeV), or ^{210}Po ($E_\alpha = 5.407$ MeV) [70]. The velocity of such an α particle is

$$\frac{v_{a,0}}{c} = \frac{\sqrt{E_{a,0}(E_{a,0}+2m_ac^2)}}{E_{a,0}+m_ac^2} \simeq 0.052, \tag{130}$$

using the α particle mass $m_ac^2 = 3727$ MeV [48], and relativistic effects are thus negligible. The α particle is assumed to mainly interact with the electrons of the medium. Indeed, the fact that the slowdown of a fast particle is mainly due to collisions with electrons is well known and is true for any material including ordinary gases such as air [32–36]. In addition, the mean electron velocity in matter is roughly given by the Bohr velocity [35,36]

$$\sqrt{\langle \mathbf{v}_b^2\rangle} \simeq \alpha c, \tag{131}$$

where $\alpha \simeq \frac{1}{137}$ is the fine-structure constant. Substituting the numerical values of Eqs. (130) and (131) into Eq. (129) leads to

$$\frac{\Lambda_\parallel}{\Lambda_\perp} \overset{t\to 0}{\simeq} 8.7. \tag{132}$$

The longitudinal elongation of the coherent wave packet is therefore significant at the start of the propagation in the particle detector.

In the long-time limit ($\eta t \gg 1$), the two coherence lengths $\Lambda_\parallel$ and $\Lambda_\perp$ tend to the same thermal wavelength

$$\Lambda_T = \frac{1}{2}\sqrt{\frac{\eta}{\xi}} = \frac{\hbar}{2\sqrt{m_ak_BT}}. \tag{133}$$

This shows that the coherent wave packet takes a spherical shape at equilibrium, as for the gas particles. In the special case of a thermal α particle at $T = 300$ K, Eq. (133) gives the value $\Lambda_T \simeq 10$ pm.

Probably one the most interesting points in Fig. 3(a) is that the transverse coherence length $\Lambda_\perp$ drops below the thermal length before rising to reach it. This results from the important effect of momentum diffusion in the transverse direction. Indeed, according to Eqs. (124) and (125), the transverse diffusion rate is much larger than the thermal one ($\gamma k_a^2 \gg \xi$) for a fast incident particle. Therefore, shortly after entering the detector, the momentum distribution of the incident particle gets more extended in the transverse direction than the thermal distribution itself, as can be seen at t_1 and t_2 in Fig. 2. In contrast, the longitudinal coherence length $\Lambda_\parallel$ does not drop below the thermal wavelength (133) according to Fig. 3(a). However, it is quite possible that, if the longitudinal decoherence term, namely, the second term on the right-hand side of Eq. (83), is retained from the beginning, the longitudinal coherence length will also manifest such an undershoot.

Finally, in order to better interpret the transverse coherence length $\Lambda_\perp$ and its time evolution for a fast particle, it is convenient to define the angular variance of the momentum distribution as

$$\langle\theta^2\rangle = \frac{K_\perp^2}{\langle \mathbf{k}_a^2\rangle}, \tag{134}$$

where $K_\perp^2$ is given by Eq. (123) and $\langle \mathbf{k}_a^2\rangle$ by Eq. (120). In the case of a fast incident particle ($v_{a,0}^2 \gg \langle \mathbf{v}_b^2\rangle$), the thermal contribution can be neglected ($\xi \to 0$) and Eq. (134) can be approximated by

$$\langle\theta^2\rangle \simeq 2\gamma t \tag{135}$$

and the transverse coherence length (128) behaves at short time as

$$\Lambda_\perp \overset{t\to 0}{\longrightarrow} \frac{1}{2k_{a,0}\langle\theta^2\rangle^{1/2}} = \frac{\lambda_{a,0}}{4\pi\langle\theta^2\rangle^{1/2}}, \tag{136}$$

where $\lambda_{a,0} = 2\pi/k_{a,0}$ is the de Broglie wavelength of the particle at the entrance in the medium. Equation (136) leads to an interesting interpretation of $\Lambda_\perp$. It corresponds to the length in the transverse direction at which the incoherent sum of plane waves rotated by the angle $\langle\theta^2\rangle^{1/2}$ is completely out of phase. This is consistent with the intuitive definition of a coherence decay length as the characteristic length for the loss of phase relation.

V. CONCLUSION

In this paper, some properties of the quantum master equation (4) governing the evolution of a fast particle in a gas (derived in a previous paper [31]) were studied in detail. We began in Sec. II with the presentation of the master equation and two of its major properties, namely, thermalization and spatial decoherence.

Then the master equation (4) was approximated in Sec. III using the quantum counterpart of the Kramers-Moyal expansion to small momentum transfer. This approximation is relevant if the particle is heavy compared to the bath scatterers or if the differential cross section is very peaked in the forward direction. The Kramers-Moyal expansion led to the general form (83) of the Caldeira-Leggett master equation valid for finite bath temperature [16,17,43–46]. This equation was then specialized to the case of strong forward scattering, resulting in Eq. (90). In particular, this equation contains a term of the double commutator of the density matrix with the angular momentum operator, which is interpreted as the transverse decoherence term applying a random infinitesimal rotation to the particle wave packet. In the Wigner representation, Eq. (90) reduces to the Fokker-Planck equation (96).

Furthermore, the coherence length of the particle was introduced and studied in Sec. IV. The coherence length matrix was defined in Eq. (99) as the covariance matrix of the off-diagonal slice of the density matrix. It was shown that, for a Gaussian state, the coherence length matrix is proportional to the inverse of the momentum covariance matrix. This property can be interpreted as a consequence of the Heisenberg uncertainty principle. In addition, it led, through the momentum variances of Eq. (123), to the time evolution of the coherence lengths in the directions parallel and perpendicular to the particle motion assuming that the transport parameters are independent of the particle energy. Since the momentum spreads more quickly in the transverse direction than in the longitudinal direction, the coherence length is smaller in the transverse direction than in the longitudinal one. Therefore, the coherent wave packet is more elongated in the direction of motion. At short time, the ratio of both is given by Eq. (129), which only depends on the velocities of the particle and the scatterers. Moreover, it turns out that the transverse coherence length drops below the thermal wavelength before reaching it after a sufficiently long time.

The original question asked by Darwin and Mott [1,2] was about the emergence of classical phenomena from plain quantum mechanics, such as the appearance of linear tracks of α particles in cloud chambers. Another important question intimately related to the previous one is the nature of the quantum state of a particle propagating in a gaseous detector. In this paper, this question was addressed within the theory of open quantum systems using the formalism of the reduced density matrix. The evolution of the density matrix is governed by quantum master equations, such as the Redfield equation (4), which reproduces many of the classical phenomena regarding the propagation of the particle, including ballistic transport, diffusion, and thermalization. In addition, these equations are able to describe fundamental quantum phenomena, in particular spatial decoherence, which is believed to play a key role in the description of measurement in quantum mechanics [10–12,19]. Decoherence manifests as the evanescence in time of the off-diagonal elements of the reduced density matrix. In this paper, it was shown that the decoherence of the particle in a gas occurs mainly in position space. Furthermore, when the cross section peaks in the forward direction, decoherence is stronger in the transverse direction than in the longitudinal direction. Therefore, the coherent wave packet should look like an ellipsoid elongated in the direction of motion. This result is quite different from the spherical coherent wave packets predicted by the Caldeira-Leggett equation, which only applies to slow Brownian particles relatively close to equilibrium with the gas. In contrast, the present paper accounts for the angular variation of the cross section, which cannot be neglected when the particle is much faster than the particles of the thermal bath. This angular variation is in particular responsible for the nontrivial shape of the coherent wave packet that was discussed above. Finally, by highlighting anisotropies in spatial decoherence, the present work achieves a significant advance in the characterization of the state of a particle undergoing quantum measurement in a detector.

Finally, an important issue that should be investigated in future works concerns the treatment of the Coulomb interaction between the α particle and the gas. When deriving the Boltzmann equation in the previous paper [31], it was assumed that the range of the interaction between the particle and the scatterers is short, but this is not the case for the Coulomb interaction, which is typically long range. Nevertheless, the Coulomb interaction is most of the time screened by the electric charges in the medium. In neutral molecules, the screening length can be of the order of the atomic Bohr radius, but, in the present context of fast particles, this length turns out to significantly exceed the atomic Bohr radius [35,36,71]. This is due to the fact that when the particle velocity is greater than the electron velocities in the medium the electrons do not have time to completely screen the electric field of the particle, resulting in long-range electric interactions between the particle and the molecules. As a consequence, the particle may interact with several molecules at a time and collective effects may occur in the medium (see [35], Chap. 5). The treatment of these effects typically resorts to dielectric linear response theory [35,72–76]. The point is that these collective effects could influence the results obtained in this paper and the previous one [31], in particular through modifications of the master equations, which suggests interesting new directions of research.

ACKNOWLEDGMENTS

The authors are grateful to Prof. Pierre Gaspard for useful suggestions and for reviewing this manuscript. The authors also thank Alban Dietrich for bringing Ref. [71] to their attention. This work was funded by the Belgian National Fund for Scientific Research (F.R.S.-FNRS) as part of the "Research Fellow" (ASP - Aspirant) fellowship program.

APPENDIX: DECOHERENCE ON A HYPERSPHERE

The purpose of this Appendix is to prove Eqs. (89) and (95) for the angular momentum operator $\hat{L}_{ij}$ under the approxima-

tion (58). Using the definition (88) of $\hat{L}_{ij}$, we write

$$\tfrac{1}{2}[\hat{L}_{ij},[\hat{L}_{ij},\hat{\rho}_a]] = \underbrace{[\hat{r}_i\hat{k}_{a,j},[\hat{r}_i\hat{k}_{a,j},\hat{\rho}_a]]}_{\hat{C}_1} - \underbrace{[\hat{r}_i\hat{k}_{a,j},[\hat{r}_j\hat{k}_{a,i},\hat{\rho}_a]]}_{\hat{C}_2}, \tag{A1}$$

where the implicit summation of repeated indices is used. Note the order of the indices i and j on the right-hand side of Eq. (A1). This double commutator of $\hat{\rho}_a$ with $\hat{L}_{ij}$ represents the transverse decoherence of the particle due to the change of direction caused by the collisions. First, let us consider the term called $\hat{C}_1$. Expanding the nested commutators leads to

$$\begin{aligned}\hat{C}_1 &= [\hat{r}_i\hat{k}_{a,j},[\hat{r}_i\hat{k}_{a,j},\hat{\rho}_a]]\\ &= \hat{r}_i\hat{k}_{a,j}\hat{r}_i\hat{k}_{a,j}\hat{\rho}_a - 2\hat{r}_i\hat{k}_{a,j}\hat{\rho}_a\hat{r}_i\hat{k}_{a,j} + \hat{\rho}_a\hat{r}_i\hat{k}_{a,j}\hat{r}_i\hat{k}_{a,j}.\end{aligned} \tag{A2}$$

Since $\hat{\rho}_a$ is assumed to be quasidiagonal in the momentum basis according to Eq. (58), it is appropriate to move the wave-vector components closer to $\hat{\rho}_a$ using the canonical commutation relation

$$[\hat{r}_i,\hat{k}_{a,j}] = i\delta_{ij}. \tag{A3}$$

Applying this idea to the first two terms of Eq. (A2) yields

$$\hat{C}_1 = \hat{r}_i\hat{r}_i\hat{\mathbf{k}}_a^2\hat{\rho}_a - 2\hat{r}_i\hat{\mathbf{k}}_a^2\hat{\rho}_a\hat{r}_i - 3i\hat{r}_i\hat{k}_{a,i}\hat{\rho}_a + \hat{\rho}_a\hat{r}_i\hat{k}_{a,j}\hat{r}_i\hat{k}_{a,j}. \tag{A4}$$

The last term of Eq. (A4) needs three commutations of the position and the momentum. The result is

$$\begin{aligned}\hat{\rho}_a\hat{r}_i\hat{k}_{a,j}\hat{r}_i\hat{k}_{a,j} &= \hat{\rho}_a(\hat{k}_{a,j}\hat{r}_i + i\delta_{ij})(\hat{k}_{a,j}\hat{r}_i + i\delta_{ij})\\ &= \hat{\rho}_a\hat{k}_{a,j}\hat{r}_i\hat{k}_{a,j}\hat{r}_i + 2i\hat{\rho}_a\hat{k}_{a,i}\hat{r}_i - \hat{\rho}_a d\\ &= \hat{\rho}_a\hat{\mathbf{k}}_a^2\hat{r}_i\hat{r}_i + 3i\hat{\rho}_a\hat{k}_{a,i}\hat{r}_i - \hat{\rho}_a d.\end{aligned} \tag{A5}$$

Then, substituting the result (A5) back into Eq. (A4) gives

$$\hat{C}_1 = \big[\hat{r}_i,\big[\hat{r}_i,\hat{\mathbf{k}}_a^2\hat{\rho}_a\big]\big] - 3i[\hat{r}_i,\hat{k}_{a,i}\hat{\rho}_a] - \hat{\rho}_a d. \tag{A6}$$

Note that between Eqs. (A4) and (A6), the assumption $[\hat{\mathbf{k}}_a,\hat{\rho}_a] \simeq 0$ has been used. The term called $\hat{C}_2$ in Eq. (A1) can be calculated in the same way, but leads to a markedly different result. Expanding the double commutator leads to

$$\begin{aligned}\hat{C}_2 &= [\hat{r}_i\hat{k}_{a,j},[\hat{r}_j\hat{k}_{a,i},\hat{\rho}_a]]\\ &= \hat{r}_i\hat{k}_{a,j}\hat{r}_j\hat{k}_{a,i}\hat{\rho}_a - 2\hat{r}_i\hat{k}_{a,j}\hat{\rho}_a\hat{r}_j\hat{k}_{a,i} + \hat{\rho}_a\hat{r}_i\hat{k}_{a,j}\hat{r}_j\hat{k}_{a,i}.\end{aligned} \tag{A7}$$

As before, we commute the positions and momenta in order to get the momenta closer to $\hat{\rho}_a$:

$$\begin{aligned}\hat{C}_2 =& \hat{r}_i\hat{r}_j\hat{k}_{a,i}\hat{k}_{a,j}\hat{\rho}_a - i(d+2)\hat{r}_i\hat{k}_{a,i}\hat{\rho}_a\\ &- 2\hat{r}_i\hat{k}_{a,i}\hat{k}_{a,j}\hat{\rho}_a\hat{r}_j + \hat{\rho}_a\hat{r}_i\hat{k}_{a,j}\hat{r}_j\hat{k}_{a,i}.\end{aligned} \tag{A8}$$

The last term of Eq. (A4) needs also three commutation steps. They read

$$\begin{aligned}\hat{\rho}_a\hat{r}_i\hat{k}_{a,j}\hat{r}_j\hat{k}_{a,i} &= \hat{\rho}_a(\hat{k}_{a,j}\hat{r}_i + i\delta_{ij})(\hat{k}_{a,i}\hat{r}_j + i\delta_{ij})\\ &= \hat{\rho}_a\hat{k}_{a,j}\hat{r}_i\hat{k}_{a,i}\hat{r}_j + 2i\hat{\rho}_a\hat{k}_{a,i}\hat{r}_i - \hat{\rho}_a d\\ &= \hat{\rho}_a\hat{k}_{a,i}\hat{k}_{a,j}\hat{r}_i\hat{r}_j + i(d+2)\hat{\rho}_a\hat{k}_{a,i}\hat{r}_i - \hat{\rho}_a d.\end{aligned} \tag{A9}$$

Inserting Eq. (A9) back into Eq. (A8) leads to the result

$$\hat{C}_2 = [\hat{r}_i,[\hat{r}_j,\hat{k}_{a,i}\hat{k}_{a,j}\hat{\rho}_a]] - i(d+2)[\hat{r}_i,\hat{k}_{a,i}\hat{\rho}_a] - \hat{\rho}_a d. \tag{A10}$$

Finally, combining Eqs. (A6) and (A10) into Eq. (A1), we obtain the sought property

$$\begin{aligned}\tfrac{1}{2}[\hat{L}_{ij},[\hat{L}_{ij},\hat{\rho}_a]] =& \big[\hat{r}_i,\big[\hat{r}_j,\big(\hat{\mathbf{k}}_a^2\delta_{ij} - \hat{k}_{a,i}\hat{k}_{a,j}\big)\hat{\rho}_a\big]\big]\\ &+ i(d-1)[\hat{r}_i,\hat{k}_{a,i}\hat{\rho}_a],\end{aligned} \tag{A11}$$

which is used in Eq. (89).

We still have to determine the effect of the double commutator of $\hat{\rho}_a$ with $\hat{L}_{ij}$ in the Wigner representation, since this representation is used in Sec. III B 2. Because of the quasidiagonality of $\hat{\rho}_a$ in the momentum basis, it is related to the Wigner function $f_a(\mathbf{k}_a)$ by

$$\hat{\rho}_a \simeq (2\pi)^d \int_{\mathbb{R}^d} d\mathbf{k}_a f_a(\mathbf{k}_a)|\mathbf{k}_a\rangle\langle\mathbf{k}_a|. \tag{A12}$$

An important consequence is that the commutators with $\hat{L}_{ij}$ reduce to a multiplication by $\hat{L}_{ij}$ in the Wigner representation

$$\mathcal{W}\big(\tfrac{1}{2}[\hat{L}_{ij},[\hat{L}_{ij},\hat{\rho}_a]]\big) = \tfrac{1}{2}\hat{L}_{ij}\hat{L}_{ij}f_a. \tag{A13}$$

It should be noted that on the right-hand side of Eq. (A13), the two operators $\hat{L}_{ij} = \hat{r}_i\hat{k}_{a,j} - \hat{r}_j\hat{k}_{a,i}$ implicitly assume that

$$\hat{r}_i = i\frac{\partial}{\partial k_{a,i}}, \quad \hat{k}_{a,i} = k_{a,i}. \tag{A14}$$

Of course, these equalities follow from the principle of correspondence in quantum mechanics. They are expressed in the momentum basis, and not in the position basis, because of the quasidiagonality of $\hat{\rho}_a$ assumed in Eq. (A12). The scalar product of angular momenta can now be expanded from the definition (88). Using the canonical commutation relation, it is relatively straightforward to get

$$\tfrac{1}{2}\hat{L}_{ij}\hat{L}_{ij} = \hat{\mathbf{k}}_a^2\hat{\mathbf{r}}^2 - (\hat{\mathbf{k}}_a\cdot\hat{\mathbf{r}})^2 - i(d-2)\hat{\mathbf{k}}_a\cdot\hat{\mathbf{r}}. \tag{A15}$$

The equalities in Eq. (A14) directly lead to

$$\tfrac{1}{2}\hat{L}_{ij}\hat{L}_{ij} = -k_a^2\nabla_{\mathbf{k}_a}^2 + (\mathbf{k}_a\cdot\boldsymbol{\nabla}_{\mathbf{k}_a})^2 + (d-2)\mathbf{k}_a\cdot\boldsymbol{\nabla}_{\mathbf{k}_a}. \tag{A16}$$

Using the fact that $\mathbf{k}_a\cdot\boldsymbol{\nabla}_{\mathbf{k}_a} = k_a\partial_{k_a}$, we get

$$\tfrac{1}{2}\hat{L}_{ij}\hat{L}_{ij} = -k_a^2\nabla_{\mathbf{k}_a}^2 + k_a^2\frac{\partial^2}{\partial k_a^2} + (d-1)k_a\frac{\partial}{\partial k_a}. \tag{A17}$$

The last step is to expand the Laplacian operator in spherical coordinates [54]

$$\nabla_{\mathbf{k}_a}^2 = \frac{\partial^2}{\partial k_a^2} + \frac{d-1}{k_a}\frac{\partial}{\partial k_a} + \frac{1}{k_a^2}\nabla_{\perp\mathbf{k}_a}^2, \tag{A18}$$

where $\nabla_{\perp\mathbf{k}_a}^2$ denotes the spherical Laplacian, which acts only on the unit hypersphere in the space $\mathcal{R}^d$. Substituting Eq. (A18) into Eq. (A17) yields

$$\tfrac{1}{2}\hat{L}_{ij}\hat{L}_{ij} = -\nabla_{\perp\mathbf{k}_a}^2. \tag{A19}$$

This result shows that the action of the double commutator in Eq. (A13) corresponds to a spherical Laplacian in the momentum space. This also proves Eq. (95).

[1] C. G. Darwin, Proc. R. Soc. A **124**, 375 (1929).
[2] N. F. Mott, Proc. R. Soc. A **126**, 79 (1929).
[3] C. Cacciapuoti, R. Carlone, and R. Figari, J. Phys. A: Math. Theor. **40**, 249 (2007).
[4] C. Cacciapuoti, R. Carlone, and R. Figari, Rep. Math. Phys. **59**, 337 (2007).
[5] R. Figari and A. Teta, *Quantum Dynamics of a Particle in a Tracking Chamber*, SpringerBriefs in Physics (Springer, New York, 2014).
[6] R. Carlone, R. Figari, and C. Negulescu, Commun. Comput. Phys. **18**, 247 (2015).
[7] G. Dell'Antonio, R. Figari, and A. Teta, J. Math. Phys. **49**, 042105 (2008).
[8] J.-M. Sparenberg and D. Gaspard, Found. Phys. **48**, 429 (2018).
[9] D. Gaspard and J.-M. Sparenberg, Int. J. Quantum Inf. **17**, 1941004 (2019).
[10] H. D. Zeh, Found. Phys. **1**, 69 (1970).
[11] H. D. Zeh, Found. Phys. **3**, 109 (1973).
[12] E. Joos and H. D. Zeh, Z. Phys. B **59**, 223 (1985).
[13] K. Hornberger and J. E. Sipe, Phys. Rev. A **68**, 012105 (2003).
[14] K. Hornberger, Phys. Rev. Lett. **97**, 060601 (2006).
[15] K. Hornberger, Europhys. Lett. **77**, 50007 (2007).
[16] K. Hornberger, in *Entanglement and Decoherence: Foundations and Modern Trends*, edited by A. Buchleitner, C. Viviescas, and M. Tiersch, Lecture Notes in Physics Vol. 768 (Springer, Berlin, 2009), Chap. 5.
[17] B. Vacchini and K. Hornberger, Phys. Rep. **478**, 71 (2009).
[18] M. R. Gallis and G. N. Fleming, Phys. Rev. A **42**, 38 (1990).
[19] W. H. Zurek, Phys. Today **44**(10), 36 (1991).
[20] W. H. Zurek, Rev. Mod. Phys. **75**, 715 (2003).
[21] A. E. Allahverdyan, R. Balian, and T. M. Nieuwenhuizen, Phys. Rep. **525**, 1 (2013).
[22] M. Schlosshauer, Phys. Rep. **831**, 1 (2019).
[23] M. Arndt, O. Nairz, J. Voss-Andreae, C. Keller, G. Van-Der-Zouw, and A. Zeilinger, Nature (London) **401**, 680 (1999).
[24] K. Hornberger, S. Uttenthaler, B. Brezger, L. Hackermüller, M. Arndt, and A. Zeilinger, Phys. Rev. Lett. **90**, 160401 (2003).
[25] L. Hackermüller, K. Hornberger, B. Brezger, A. Zeilinger, and M. Arndt, Nature (London) **427**, 711 (2004).
[26] T. Juffmann, H. Ulbricht, and M. Arndt, Rep. Prog. Phys. **76**, 086402 (2013).
[27] S. Eibenberger, S. Gerlich, M. Arndt, M. Mayor, and J. Tüxen, Phys. Chem. Chem. Phys. **15**, 14696 (2013).
[28] Y. Y. Fein, P. Geyer, P. Zwick, F. Kiałka, S. Pedalino, M. Mayor, S. Gerlich, and M. Arndt, Nat. Phys. **15**, 1242 (2019).
[29] C. Brand, F. Kiałka, S. Troyer, C. Knobloch, K. Simonović, B. A. Stickler, K. Hornberger, and M. Arndt, Phys. Rev. Lett. **125**, 033604 (2020).
[30] B. Schrinski, S. Nimmrichter, and K. Hornberger, Phys. Rev. Res. **2**, 033034 (2020).
[31] D. Gaspard, Phys. Rev. A **106**, 062211 (2022).
[32] J. Ashkin, K. T. Bainbridge, H. A. Bethe, N. F. Ramsey, and H. H. Staub, in *Experimental Nuclear Physics*, Volume 1, edited by E. Segrè (Wiley, New York, 1953).
[33] E. G. Segrè, *Nuclei and Particles: An Introduction to Nuclear and Subnuclear Physics*, 2nd ed. (Benjamin, Reading, 1977).
[34] J. F. Ziegler and J. P. Biersack, in *Treatise on Heavy-Ion Science*, Volume 6, edited by D. A. Bromley (Springer, Boston, 1985), Chap. 3.
[35] P. Sigmund, *Particle Penetration and Radiation Effects: General Aspects and Stopping of Swift Point Charges*, 1st ed., Springer Series in Solid-State Sciences Vol. 151 (Springer, Berlin, 2006).
[36] P. Sigmund, *Particle Penetration and Radiation Effects Volume 2 Penetration of Atomic and Molecular Ions*, 1st ed., Springer Series in Solid-State Sciences Vol. 179 (Springer, Cham, 2014).
[37] A. Wax and J. E. Thomas, J. Opt. Soc. Am. A **15**, 1896 (1998).
[38] C.-C. Cheng and M. G. Raymer, Phys. Rev. Lett. **82**, 4807 (1999).
[39] H. A. Kramers, Physica **7**, 284 (1940).
[40] J. E. Moyal, J. R. Stat. Soc. B **11**, 150 (1949).
[41] H. Akama and A. Siegel, Physica **31**, 1493 (1965).
[42] R. F. Pawula, Phys. Rev. **162**, 186 (1967).
[43] A. O. Caldeira and A. J. Leggett, Physica A **121**, 587 (1983).
[44] L. Diósi, Physica A **199**, 517 (1993).
[45] H.-P. Breuer and F. Petruccione, *The Theory of Open Quantum Systems* (Oxford University Press, Oxford, 2002).
[46] I. Kamleitner, Open quantum system dynamics from a measurement perspective: Applications to coherent particle transport and to quantum Brownian motion, Ph.D. thesis, Macquarie University, 2010.
[47] S. M. Barnett, S. Franke-Arnold, A. S. Arnold, and C. Baxter, J. Phys. B **33**, 4177 (2000).
[48] E. Tiesinga, P. J. Mohr, D. B. Newell, and B. N. Taylor, Rev. Mod. Phys. **93**, 025010 (2021).
[49] P. Sheng, *Introduction to Wave Scattering, Localization and Mesoscopic Phenomena*, Springer Series in Materials Science Vol. 88 (Springer, Berlin, 2006).
[50] E. Akkermans and G. Montambaux, *Mesoscopic Physics of Electrons and Photons*, 1st ed. (Cambridge University Press, Cambridge, 2007).
[51] A. M. Weinberg and E. P. Wigner, *The Physical Theory of Neutron Chain Reactors* (University of Chicago Press, Chicago, 1958).
[52] M. J. Berger, J. S. Coursey, and M. A. Zucker, ESTAR, PSTAR, and ASTAR: Computer programs for calculating stopping-power and range tables for electrons, protons, and helium ions, NIST Standard Reference Database 124, available at https://physics.nist.gov/Star (2017), updated by S. M. Seltzer and P. M. Bergstrom.
[53] S. L. Adler, J. Phys. A: Math. Gen. **39**, 14067 (2006).
[54] F. W. J. Olver, D. W. Lozier, R. F. Boisvert, and C. W. Clark, *NIST Handbook of Mathematical Functions*, 1st ed. (Cambridge University Press, Cambridge, 2010).
[55] K. Huang, *Statistical Mechanics*, 2nd ed. (Wiley, New York, 1987).
[56] L. D. Landau and E. M. Lifshitz, *Quantum Mechanics: Non-Relativistic Theory*, 2nd ed., Course of Theoretical Physics Vol. 3 (Mir, Moscow, 1967).
[57] E. P. Wigner, Phys. Rev. **40**, 749 (1932).
[58] J. E. Moyal, Math. Proc. Cambridge Philos. Soc. **45**, 99 (1949).
[59] J.-L. Basdevant and J. Dalibard, *Quantum Mechanics* (Springer, Berlin, 2002).
[60] C. Cohen-Tannoudji, B. Diu, and F. Laloë, *Quantum Mechanics, Volume 3 Fermions, Bosons, Photons, Correlations, and Entanglement*, 1st ed. (Wiley, Weinheim, 2020).
[61] L. Diósi, Europhys. Lett. **30**, 63 (1995).
[62] W. Heisenberg, Z. Phys. **43**, 172 (1927).
[63] A. Messiah, *Quantum Mechanics*, Volume 1 (Interscience, New York, 1961).

[64] B. C. Hall, *Quantum Theory for Mathematicians*, Graduate Texts Mathematics Vol. 267 (Springer, New York, 2013).
[65] V. B. Braginsky and F. Y. Khalili, in *Quantum Measurement*, edited by K. S. Thorne (Cambridge University Press, Cambridge, 1992).
[66] W. H. Bragg and R. Kleeman, Philos. Mag. **10**, 318 (1905).
[67] E. Rutherford, Sci. Mon. **18**, 337 (1924).
[68] M. S. Livingston and H. A. Bethe, Rev. Mod. Phys. **9**, 245 (1937).
[69] M.-M. Bé, V. Chisté, C. Dulieu, E. Browne, C. Baglin, V. Chechev, N. Kuzmenco, R. Helmer, F. Kondev, D. McMahon, and K. B. Lee, *Table of Radionuclides (Vol. 3 - A = 3 to 244)* (BIPM, Sèvres, 2006).
[70] M.-M. Bé, V. Chisté, C. Dulieu, E. Browne, V. Chechev, N. Kuzmenko, F. G. Kondev, A. Luca, M. Galán, A. Pearce, and X. Huang, *Table of Radionuclides (Vol. 4 - A = 133 to 252)* (BIPM, Sèvres, 2008).
[71] A. F. Lifschitz and N. R. Arista, Phys. Rev. A **57**, 200 (1998).
[72] I. E. Tamm, in *Selected Papers*, edited by B. M. Bolotovskii, V. Y. Frenkel, and R. Peierls (Springer, Berlin, 1991), papers E.1 and E.2.
[73] E. Fermi, Phys. Rev. **56**, 1242 (1939).
[74] E. Fermi, Phys. Rev. **57**, 485 (1940).
[75] A. Bohr, Mat. Fys. Medd. **24**, 19 (1948).
[76] O. Halpern and H. Hall, Phys. Rev. **73**, 477 (1948).